

Clownfish metapopulation persistence draft

Allison G. Dedrick^{a,*}

Katrina A. Catalano^a

Michelle R. Stuart^a

J. Wilson White^b

Humberto Montes, Jr.^c

Malin Pinsky^a

a. Department of Ecology Evolution and Natural Resources, Rutgers University, 14 College Farm Road, New Brunswick, NJ 08901;

b. Oregon State University

c. Visayas State University

* Corresponding author; e-mail: agdedrick@gmail.com

(Author order not yet determined)

Introduction

Metapopulations exist along a continuum, with dynamics driven by the balance of extinction and colonization of local patches at one extreme and the balance of immigration at the other. In this paper, we focus on the balance of extinction and colonization, which is often referred to as the balance of dispersal. We will show that the balance of dispersal can be used to predict the persistence of a metapopulation.

tion and emmigration at constantly-occupied local patches at the other (Kritzer and Sale, 2006). Terrestrial metapopulations often show extinction-colonization dynamics (e.g. Hanski, 1998), while marine metapopulations tend to exhibit immigration-
emmigration dynamics where local extinction of patches is uncommon (Kritzer and Sale, 2006). For these metapopulations, dynamics and persistence depend on connectivity among patches and the demographic rates at each patch (e.g. Hastings and Botsford, 2006a; Hanski, 1998). Assessing levels of connectivity and demographic parameters has been particularly challenging for marine species, where much of the mortality and movement happens at larval and juvenile stages when individuals are hard to track and have the potential to travel long distances with ocean currents (e.g. Kritzer and Sale, 2006; Cowen and Sponaugle, 2009; Roughgarden et al., 1988).

A need to understand metapopulations for conservation and management, such as siting marine protected areas (e.g. Botsford et al., 2001; White et al., 2010), however, has led to a large body of theory describing how marine metapopulations might persist.

For any population to persist, individuals must on average replace themselves during their lifetime. Assessing replacement must take into account the demographic processes across the whole life cycle, including how likely individuals are to survive to the next age or stage, their expected fecundity at each stage, and the survival of any offspring produced to recruitment. In a spatially-structured population, as many marine populations are, in addition to assessing whether the reproductive output and survival of a population is sufficient, we must also consider how the offspring are distributed across space.

27 Considering both the demographic processes within patches and the connectivity
among them, a metapopulation can persist in two ways: 1) at least one patch can
achieve replacement in isolation, or 2) patches receive enough recruitment to achieve
30 replacement through multi-generational loops of connectivity with other patches in
the metapopulation (Hastings and Botsford, 2006a; Burgess et al., 2014). In the first
case (termed self-persistence), enough of the reproductive output produced at one
33 patch is retained at the patch for it to persist. In the second (network persistence),
closed loops of connectivity among at least some of the patches - where individuals
from one patch settle at another and eventually send offspring back to the first in a
36 future generation - provide the patch with enough recruitment to persist within the
network. Though it has been challenging to estimate the parameters necessary to
understand how actual metapopulations persist, a large work of theory developed in
39 part to guide marine protected area design helps predict when each type of persistence
is likely to occur (i.e., large patches relative to the mean dispersal distance are likely
to be self-persistent, Botsford et al., 2001).

42 New ways of identifying individuals and determining their origins, such as otolith
and shell microchemistry and genetic parentage analysis (e.g. Wang, 2004, 2014) are
making it increasingly possible to estimate both the demographic (e.g. Carson et al.,
45 2011; Hameed et al., 2016) and the dispersal (e.g. Almany et al., 2017; D'Aloia et al.,
2013) parameters necessary to assess persistence in real metapopulations. We might
expect that populations on isolated islands are the most likely to be self-persistent,
48 as they lack nearby populations with which to exchange larvae and would go locally
extinct if they did not achieve replacement. At isolated Kimbe Island in Papua New

Guinea, Salles et al. (2015) find that the population of orange clownfish (*Amphiprion percula*) can likely persist without outside immigration. In contrast, populations of bicolor damselfish (*Stegastes partitus*) at a set of reef patches across four isolated islands in the Bahamas do not appear able to persist without outside input (Johnson et al., 2018). For populations that exist in patches along a continuous linear coastline, rather than on separate islands, however, the scale of metapopulation persistence is still an open question.

The number of studies estimating demographic rates and connectivity in marine metapopulations is growing (e.g. Carson et al., 2011; Salles et al., 2015; Johnson et al., 2018; Garavelli et al., 2018), but most use data from one or a few years. Longer data sets enable better estimates of long-term average rates, rather than assuming the demographic and dispersal rates from a particular year or two are representative. Long data set are also useful for explicitly considering uncertainty, both to assess how well we understand persistence for a population and to assess which parameters contribute most to our uncertainty. Finally, sampling over many years provides abundance trends to compare with persistence metrics.

Here, we further our understanding of metapopulation dynamics in a network of patches along a coastline through a study of yellowtail clownfish (*Amphiprion clarkii*) in the Philippines. We assess persistence for all patches of habitat within a 30 km stretch of coastline, exceeding estimates of the dispersal spread for this species (Pinsky et al., 2010), suggesting the network is likely to operate as a contained metapopulation. With seven years of annual sampling data, we are able to estimate persistence metrics and replacement over the longer term and investigate abundance

through time to compare with the replacement-based persistence metrics. We use our long-term data set from habitat patches on a continuous section of coastline to
75 understand persistence within a local network.

Methods

Persistence theory and metrics

78 For a population to persist, individuals must be able to replace themselves on average at low abundance (e.g. Hastings and Botsford, 2006a; Botsford et al., 2009). In non-spatially structured populations, we use criteria such as the average number
81 of recruiting offspring each individual produces during its life (called R_0 when the population is age-structured and density-independent) or the growth rate of the population (such as the dominant eigenvalue λ of an age-structured Leslie matrix) (Caswell, 2001; Burgess et al., 2014). For spatially-structured populations, we must
84 also consider the spatial spread of offspring, often represented through a dispersal kernel or connectivity matrix (e.g. Cowen, 2006; Buston et al., 2011; Hogan et al.,
87 2011; DAloia et al., 2015)).

We consider four primary metrics to assess whether and how the population is persistent: 1) lifetime recruit production (LRP), to assess whether the population
90 has enough surviving offspring to achieve replacement, 2) self-persistence (SP), to assess whether any individual patch can persist in isolation without input from other patches, 3) network persistence (NP), to assess whether the metapopulation is per-
93 sistent as a connected unit, and 4) local replacement (LR), as another assessment of

whether individuals replace themselves with recruits retained within population. We
explain each metric below in detail. To represent the uncertainty in our estimates, we
96 calculate each metric 1000 times, pulling each input parameter from a distribution
or range. In our results, we show the range of values of each persistence metric as
well as our best estimate.

99 **Lifetime recruit production**

We find the estimated number of recruits an individual recruit will produce (lifetime
recruit production: LRP) by multiplying the total number of eggs a recruit-sized
102 individual will produce in its lifetime (lifetime egg production: LEP) by the fraction
of those eggs that will survive to become recruits (egg-recruit survival: S_e) (Fig. 2):

$$105 \quad \text{LRP} = \text{LEP} * S_e. \quad (1)$$

If $LRP \geq 1$, the population has the potential for replacement; individuals produce
105 enough surviving offspring, before taking into account dispersal. If $LRP < 1$, the
individuals are not replacing themselves and the population cannot persist without
input from outside patches. We use all recruits produced by adults in our population,
108 regardless of where they settle, to estimate LRP .

Self-persistence

A patch is able to persist in isolation (self-persistent) if individuals produce enough
111 offspring that survive to recruitment (LRP) and settle in the natal patch (with

probability of dispersal $p_{i,i}$) to replace themselves.

$$SP_i = \text{LRP} \times p_{i,i}, \quad (2)$$

where $p_{i,i}$ is the probability that a recruit born in patch i will settle in patch i ,
114 given that it survives to recruit somewhere.

A patch is self-persistent if $SP \geq 1$. If at least one patch is self-persistent, the metapopulation as a whole is persistent as well (Hastings and Botsford, 2006a; 117 Burgess et al., 2014). Our equation for SP is a modification of that used in Burgess et al. (2014), which uses LEP to represent offspring produced and uses local retention - the number of surviving recruits that disperse back to the natal patch divided the 120 number of eggs produced by the natal patch - to capture egg-recruit survival and dispersal combined: $\text{LEP} \times \text{local retention} \geq 1$. We modify this to include egg-recruit survival in the offspring term, using LRP in place of LEP, to assess whether 123 a particular patch i is self-persistent.

Network persistence

In addition to the production of each site, network persistence explicitly considers 126 dispersal of individuals among sites, which is a critical part of the larval life stage. We represent dispersal with a dispersal kernel, which relates the likelihood of an individual traveling to distanced traveled. We find the probabilities of a recruit dispersing 129 between each set of sites ($p_{i,j}$) by integrating the dispersal kernel over the distances

between sites. We then create a realized connectivity matrix C by multiplying the dispersal probabilities by the expected number of recruits an individual produces:

132 $C_{i,j} = \text{LRP} \times p_{i,j}$ (Burgess et al., 2014, though we include egg-recruit survival in LRP, rather than in $p_{i,j}$ as they do). The diagonal entries of C , where the origin and destination are the same site, are the values of self-persistence for each individual

135 site.

Network persistence evaluates the largest real eigenvalue of the realized connectivity matrix λ_C , which must be greater than 1 for the network to persist without outside input: $\text{NP} = \lambda_C > 1$ (e.g. Hastings and Botsford, 2006a; White et al., 2010; Burgess et al., 2014).

Local replacement

141 Like network persistence, local replacement (LR) assesses whether the population is locally self-sustaining. Rather than considering dispersal explicitly as network persistence does, local replacement modifies LRP to estimate the average number of recruits produced per individual that return to settle within our sites. We estimate 144 LR by multiplying LEP by the proportion of eggs produced that survive and return to recruit at our sites (R_e), a modification of egg-recruit survival. If $LR \geq 1$, individuals produce enough locally-retained offspring to replace themselves and the population 147 can persist in isolation.

$$\text{LR} = \text{LEP} \times R_e. \quad (3)$$

Study system

We focus on a tropical metapopulation of yellowtail clownfish (*Ampiprion clarkii*, Fig. 3c) on the west coast of Leyte island facing the Camotes Sea in the Philippines (Fig. 3a). Like many clownfish species, yellowtail clownfish have a mutualistic relationship with anemones that house small colonies of fish (Buston, 2003b; Fautin et al., 1992). Yellowtail clownfish are protandrous hermaphrodites and maintain a size-structured hierarchy; within an anemone, the largest fish is the breeding female, the next largest is the breeding male, and any smaller fish are non-breeding juveniles. The fish move up in rank to become breeders only after the larger fish have died. In the tropical patch reef habitat of the Philippines, yellowtail clownfish primarily spawn from November to May, laying clutches of benthic eggs that the parents protect and tend (Ochi, 1989; Holtswarth et al., 2017). Larvae hatch after about six days and spend 7-10 days in the water column before returning to reef habitat to settle in an anemone (Fautin et al., 1992).

Clownfish are particularly well-suited to metapopulation studies due to their limited movement as adults and clearly patchy habitat. Once fish have settled, they tend to stay within close proximity of their anemones, which are found on reef patches. This makes fish easier to relocate for mark-recapture studies and simplifies the exchange between patches to only dispersal during the larval phase. Patches, whether considered to be the reef patch or the anemone territory of the fish, are clearly discrete and easily delineated (Fig. 3a, b), which makes determining the spatial structure of the metapopulation clear. Additionally, clear patches make it easier to assess how

¹⁷¹ much of the site has been surveyed. These simplifying characteristics in habitat and
fish behavior make clownfish and other similarly territorial reef fish useful model
systems for studies of metapopulation dynamics and persistence (e.g. Buston and
¹⁷⁴ DAloia, 2013; Salles et al., 2015; Johnson et al., 2018). Our focal species of yellowtail
clownfish tends to behave more like larger reef fishes, with wider-ranging territories
and stronger swimming abilities (Hattori and Yanagisawa, 1991; Ochi, 1989), than
¹⁷⁷ the smaller clownfish *A. percula* commonly used in previous metapopulation studies
(e.g. Buston et al., 2011; Salles et al., 2015). As we show later, survival in yellow-
tail clownfish is also lower than *A. percula* and more similar to other damselfishes.
¹⁸⁰ MAKE SURE THIS SENTENCE IS TRUE!

Field data collection

We focus on a set of seventeen patch reef sites spanning 30 km along the western coast
¹⁸³ of Leyte island (Fig. 3a). The sites consist of rocky patches of coral reef separated
by sand flats (Fig. 3b). On the north edge, the sites are isolated from nearby habitat
with no substantial reef habitat for at least 20 km.

¹⁸⁶ Since 2012, we have sampled fish and habitat at most of the sites annually (Table
A2). During sampling, divers using SCUBA and tethered to GPS readers swam the
extent of each site. Divers visited each anemone inhabited by yellowtail clownfish
¹⁸⁹ and tagged anemones. At each anemone, the divers attempted to catch all of the
yellowtail clownfish 3.5 cm and larger, took a small tail fin-clip from each for use in
genetic analysis, measured the fork length, and noted the tail color (as an indicator of
¹⁹² life stage). Starting in the 2015 field season, fish 6.0 cm and larger were also tagged

with a passive integrated transponder (PIT) tag, unless already tagged. Divers also looked for eggs around each anemone and measured and photographed any clutches found. In total, we took fin clips from and genotyped 2772 fish and PIT-tagged 1929 fish across all years and sites combined, marking 3413 individual fish.

198 Estimating demographic and dispersal parameters from empirical data

Parentage analysis and dispersal kernel

We use a distance-based dispersal kernel fit from parent-offspring matches ((Catalano et al., in prep)), where the relative dispersal is a function of distance d in kilometers and parameters $\theta = 1.19$ and $z = e^{k_d=-2.33}$ that control the shape and scale of the kernel. The dispersal kernel is estimated using fish that have already recruited to a population and survived to be sampled so includes only the probability of dispersing, not pre-settlement mortality. To find the probability of fish dispersing among our sites, we numerically integrate the dispersal kernel using the distance from the middle of the origin site (i) to the closest (d_1) and farthest (d_2) bounds of the destination site (j):

$$p_{i,j}(d) = \int_{d_1}^{d_2} z e^{-(zd)^\theta} dd. \quad (4)$$

To account for uncertainty in the dispersal kernel, we use sets of the shape parameter θ and the scale parameter k_d that represent the span of the 95% confidence interval.

Growth and survival: mark-recapture analyses

213 We marked fish with both genetic samples and PIT tags, allowing us to estimate growth and survival through mark-recapture. In total, we have 3413 marked fish with size and stage data for each capture time.

216 For growth, we estimate the parameters of a von Bertalanffy growth curve (Fabens, 1965) in the growth increment form relating the length at first capture L_t to the length at a later capture L_{t+1} (Hart and Chute, 2009), where L_∞ is the average 219 asymptotic size across the population and K controls the rate of growth:

$$\begin{aligned} L_{t+1} &= L_t + (L_\infty - L_t)[1 - e^{(-K)}] \\ &= e^{(-K)}L_t + L_\infty[1 - e^{(-K)}]. \end{aligned} \tag{5}$$

We see from eqn. 5 that we would expect the first length L_t and the second length L_{t+1} to be related linearly (Hart and Chute, 2009). From the slope $m = e^{(-K)}$ and 222 y-intercept $b = L_\infty[1 - e^{(-K)}]$, we calculate the von Bertalanffy parameters, such that $K = -\ln m$ and $L_\infty = \frac{b}{(1-m)}$. We used the first and second capture lengths for fish that were recaptured after a year (within 345 to 385 days) to estimate L_∞ and 225 K . We have some fish that were recaptured more than two times so we randomly selected only one pair of recaptures from each to use in estimating the parameters, then repeated this process 1000 times to generate a set of von Bertalanffy growth 228 curves.

We use the full set of marked fish to estimate annual survival ϕ and probability

of recapture p_r using the mark-recapture program MARK implemented in R (Laake, 231 2013). We fit several models with year, size, and site effects on the probability of survival on a log-odds scale (see full list in Table A3). For fish that are not recaptured in particular year, we estimate their size using our growth model (eqn. 5) and the 234 size recorded or estimated in the previous year. Because fish are not well-mixed at our sites and instead stay quite close to their home anemones, we need to swim near an anemone to have a reasonable chance of capturing the fish on it. Therefore, we 237 also consider a distance effect on recapture probability; we use the GPS tracks of divers to estimate the minimum distance between a diver and the anemone for each tagged fish in each sample year and include it as a factor in some of the models. We 240 compared the fit of the models using AICc and selected the model with the lowest AICc value. (Table A3). ELABORATE ON AICc!!

Fecundity

243 We use a size-dependent fecundity relationship determined using photos of egg clutches and females (Yawdoszyn, in prep), where the number of eggs per clutch (E_c) is exponentially related to the length in cm of the female (L) with size effect $\beta_l = 2.388$, 246 intercept $b = 1.174$, and egg age effect $\beta_e = -0.6083$ dependent on if the eggs are old enough to have visible eyes. We multiply the number of eyed eggs per clutch by the number of clutches per year $c_e = 11.9$ (estimate from Holtswarth et al., 2017) to 249 get total annual fecundity f :

$$f = c_e * e^{\beta_l \ln(L) + \beta_e [\text{eyed}] + b}. \quad (6)$$

Lifetime egg production

We use an integral projection model (IPM) (e.g. Rees et al., 2014) with size as the continuous structuring trait z to estimate lifetime egg production (LEP), the total number of eggs produced by one recruit. We initialize the IPM with one recruit-sized individual ($\text{size}_{\text{recruit}}$) at the initial annual time step ($t = 0$), then project forward for 100 time steps using the size-dependent survival (eqn. 11) and growth (eqn. 5) functions as the probability density functions that make up the kernel to describe the survival and growth of the individual into the next time step. This gives us the size distribution at each time step, which represents the probability that the individual has survived and grown into each of the possible size categories, ranging from a minimum of $L_s = 0$ cm to a maximum of $U_s = 15$ cm divided into 100 bins.

The probability that the individual is still alive and of any size decreases as the time steps progress; by using a large number of steps, we are able to avoid arbitrarily setting a maximum age and instead let the probabilities become essentially zero.

We then multiply the size-distribution v_z at each time by the size-dependent fecundity f_z described above (eqn. 6) to get the total number of eggs produced at each time step. We then integrate across time and size to get the total number of eggs one individual is likely to produce in its lifetime:

$$\text{LEP} = \int_{t=0}^{100} \int_{z=L_s}^{z=U_s} v_{z,t} f_z dz dt. \quad (7)$$

To compute LEP, we discretize time and size and sum across the matrix. When entering the starting individual into the matrix, we use 0.1 as the standard deviation

270 of size ($\text{size}_{\text{recruit},sd}$) and estimate the standard deviation of the distribution of sizes
of fish in the next year (size_{sd}) from our recapture data (A1).

273 We only consider reproductive effort once the fish has reached the female stage
and use the average size of first observation as female for recaptured fish as the
transition size $L_f = 9.32\text{cm}$. To incorporate uncertainty, we sample directly from
the sizes at which recaptured fish were first captured as female (5.2 cm - 12.7 cm)
276 (Fig. 4d).

Survival from egg to recruit

279 We estimate survival from egg to recruit (S_e) using parentage matches to estimate
the number of surviving recruits produced by genotyped parents (similar to the
method in Johnson et al., 2018). We scale the number of offspring we match back
to parents ($R_m = 62$) by various ways we could have missed offspring (P_h , P_c , P_d ,
282 and P_s , described below), then divide by the estimated number of eggs produced by
genotyped parents, found by multiplying the number of genotyped parents ($N_g =$
1719) by the expected lifetime egg production for a fish of parent size (LEP_p):

$$S_e = \frac{\frac{R_m}{P_h P_c P_d P_s}}{N_g \text{LEP}_p}. \quad (8)$$

285 We scale the number of matched recruits we find by the cumulative proportion of
habitat in our sites we sampled over time ($P_h = 0.41$, details in A.1), the probability
of capturing a fish if we sampled its anemone ($P_c = 0.56$, see A.2 for details), and
288 the proportion of the total dispersal kernel area from each our of sites covered within

our sampling region ($P_d = 0.57$, calculation in A.2). Finally, because our dispersal kernel gives the probability of dispersal given that a recruit settled somewhere but our sampling region is not all habitat, we scale by the proportion habitat in our sampling region ($P_s = 0.20$, details in A.2.0.1) to avoid counting this mortality twice.

To estimate $\text{LRP}_{\text{local}}$, we scale only by the proportion of habitat we cumulatively sample in our sites and the probability of capturing a fish.

To incorporate uncertainty in our estimate of egg-recruit survival, we consider uncertainty in the number of offspring assigned to parents during the parentage analysis (R_m) and in the probability of capturing a fish (P_c). We generate a set of values for the number of assigned offspring using a random binomial, where the number of trials is the number of genotyped offspring (745) and the probability of success on each trial is the assignment rate of offspring from the parentage analysis (0.079) (Catalano et al., in prep). For the probability of capturing a fish, we pull values from a beta distribution that captures the mean and variance of capture probabilities across recapture dives (details in A.2).

Defining recruit and census stage

When assessing persistence, it is important to consider mortality and reproduction that occurs across the entire life cycle to determine whether an individual is replacing itself with an individual that reaches the same life stage (Burgess et al., 2014). We define a recruit to be a juvenile individual that has settled on the reef within the previous year, which also encompasses the size we are first able to sample (3.5-6.0 cm for parentage studies) (Fig. 2). In theory, it does not matter how we define recruit

as long as we use that definition in our calculations of both egg-recruit survival and
312 LEP. In our system, however, while it is straightforward to calculate LEP from any
size, we do not have enough tagged recruits to reliably estimate survival to different
recruit sizes. Instead, we choose the mean size of offspring matched in the parentage
315 study as our best estimate of the size of a recruit ($\text{size}_{\text{recruit}}$) and test sensitivity to
different recruit sizes by pulling from a uniform distribution over the sizes the recruit
stage covers (3.5-6 cm, Table A1).

318 Accounting for density-dependence

Ideally we would assess persistence metrics when the population is at low abundance
and not limited by density-dependence. Clownfish have strong social hierarchies and
321 juveniles on an anemone will prevent others from settling there as well (seen in *A.
percula*, Buston, 2003a). Each anenome, therefore, can only house one settling clown-
fish, with anemones already occupied by *A. clarkii* settlers essentially unavailable as
324 habitat. We attempt to account for this density-dependent mortality by multiply-
ing our estimate of settling recruits (the numerator of eqn. 8) by the proportional
increase (DD) in unoccupied anemones at our sites if all of the *A. clarkii* anemones
327 were unoccupied, where p_A is the proportion of anemones occupied by *A. clarkii* and
 p_U is the proportion of unoccupied anemones: $\text{DD} = \frac{(p_U + p_A)}{p_U}$. We present results
both with and without this density-dependence modification.

330 **Estimated abundance over time**

We also consider trends in abundance of breeding females at each site over time to compare to our replacement-based estimates of persistence. Similarly to as we do for offspring, we scale up the number of females caught at each site i in each sampling year t by the proportion of habitat sampled in that site and year $P_{h_i,t}$ and by the probability of capturing a fish P_c :

$$\# \text{ females}_{i,t} = \frac{\# \text{ females captured}_{i,t}}{P_{h_i,t} P_c}. \quad (9)$$

336 We then fit a linear model through the time series for each site i sampled in at least three years to assess whether the slope over time is positive or negative:

$$\# \text{ females}_i \sim \text{year} \quad (10)$$

Results

339 Our estimated abundance of females at each site over time does not suggest a clear trend (Fig. 1). In our very simple look at whether abundance seems to be increasing or decreasing, eleven sites had a positive slope over time and five had a negative slope (Fig. 1q). For the two largest sites, with a mean estimated number of females of between 150-200, one has a positive slope (Wangag, Fig. 1b) and one has a negative slope (Sitio Baybayon, Fig. 1p) and the next two largest sites are also split (Palanas, Fig. 1a and Haina, Fig. 1o). Overall, there is not a clear directional change in

abundance across the sites we sample over our sampling period.

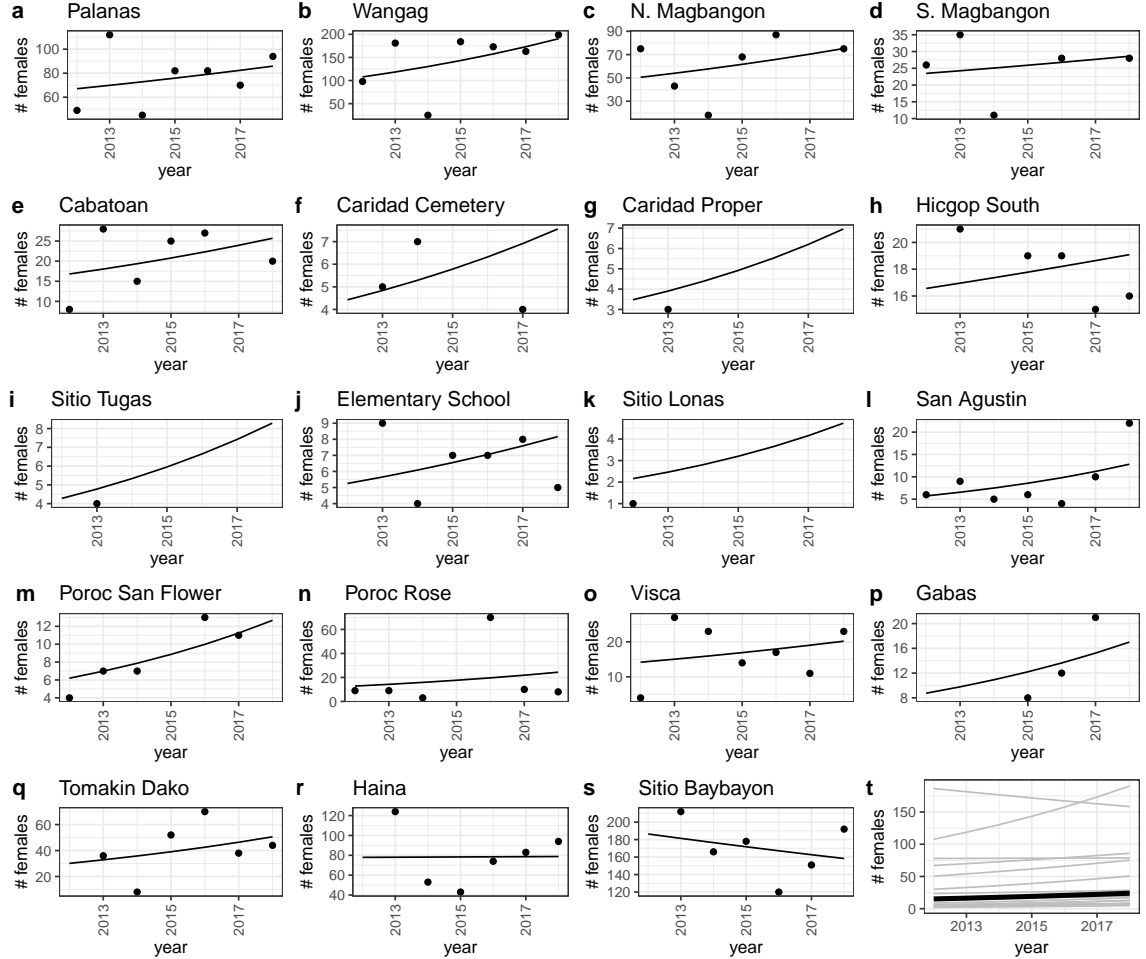


Figure 1: The estimated number of females at each site over the sampling years for sites sampled in at least three years. The total number of females at each site was estimated by scaling up the number of females captured at each site in each year by the proportion of habitat sampled at that site that season (see A.1 for details) and by the average probability of capturing a fish (see A.2). We show the estimated abundances and trend for each site individually (a-p) and a histogram of the slopes of abundance through time (q).

From the mark-recapture analysis of tagged and genotyped fish, we estimate mean

348 values of $L_\infty = 10.71\text{cm}$ (range of estimates 10.50 - 10.90 cm) and $K = 0.864$ (range
 of estimates 0.785 - 0.944) for the von Bertalanffy growth curve parameters (eqn. 5,
 Fig. 4b, Table A1). For juvenile and adult (post-recruitment) survival on a log-odds
 351 scale, the best-fit model has an effect of size, with coefficient $b_a = 0.169 \pm 0.028$ SE
 and intercept $b_\phi = -1.83 \pm 0.231$ SE (eqn. 11). The accompanying best-fit model
 for log-odds recapture probability has a negative size effect and a negative effect of
 354 diver distance from the anemone (eqn. A.3, Fig. A.4).

$$\log\left(\frac{\phi}{1-\phi}\right) = b_\phi + b_a \text{size.} \quad (11)$$

Using our best estimates for growth, survival, and fecundity, we calculate a value
 for LEP of 1061, ranging from 39 to 10345 when we consider uncertainty in the
 357 inputs (Fig. 5b). Adult survival has the most effect on the value of LEP (Fig. B.7),
 with higher values of LEP the higher annual survival of adults.

We estimate egg-recruit survival S_e to be 7.8e-04, ranging from 1.2e-04 to 0.033
 360 when we include uncertainty in the number of offspring assigned to parents and the
 probability of catching a fish (APPENDIX FIG!). When we compensate for density-
 dependence in our data, we estimate S_e to be 0.0013, ranging from 2.1e-04 to 0.057.
 363 These are somewhat high values of egg-recruit survival compared to what we see
 elsewhere in the literature (e.g. Rumrill, 1990; Metaxas and Saunders, 2009) (though
 not unreasonable, e.g. White et al., 2014; Johnson et al., 2018) because we scale up
 366 by the amount of habitat in our sampling area and count mortality due to dispersal
 to non-habitat in the dispersal probability, rather than in S_e . Uncertainty in the size

of transition to breeding female L_f has the largest effect on egg-recruit survival (Fig. 369 B.9); we only consider reproduction from females, to avoid double-counting, so the larger the transition size to female, the fewer tagged eggs we estimate were produced by genotyped parents and the higher egg-recruit survival.

372 We estimate lifetime recruit production (LRP), the product of LEP and S_e , to be 0.83, with a range of 0.28 - 3.89 when we consider uncertainty in inputs. When we compensate for density-dependence, we estimate a value of 1.42 for LRP, with a 375 range of 0.48 - 6.66. The value when we compensate for density-dependence and the range of uncertainty for both are above the threshold of one necessary for replacement before considering dispersal. This mean that individuals at our sites produce enough 378 surviving offspring before considering dispersal to be able to replace themselves, but LRP does not tell us whether those offspring will settle within our sample sites and drive persistence.

381 We also estimate replacement for recruits from our sites returning to our sites, LRP_{local} , which implicitly includes dispersal mortality, to be 0.09 (ranging from 0.03 to 0.44 when we include uncertainty) or 0.16 (0.05 to 0.76) when we compensate for 384 density-dependence. With a value well below one, this suggests individuals at our sites do not replace themselves with recruits that settle in our sites, suggesting our sites do not persist as an independent network. When we calculate LRP_{local} using all arriving recruits to our sites, however, rather than just those originating there, the best estimates are > 1 whether or not we compensate for density dependence (2.06, 1.22, respectively), suggesting that there is recruit-recruit replacement at our sites 387 when we include immigrant recruits.

We do not find any sites with $SP > 1$, whether we compensate for density-dependence or not (Fig. 6a), indicating that no site could persist in isolation. Given
393 that our best estimate of LRP does not suggest replacement and only a fraction
of those offspring stay at the natal site, this makes sense. We see the highest values
396 of self-persistence at Haina ($SP = 0.079, 0.13$ when compensating for density-
dependence) and Wangag ($SP = 0.048, 0.082$ when compensating for density-dependence),
our two widest sites.

For network persistence, our best estimate of the dominant eigenvalue of the
399 realized connectivity matrix λ_c is 0.21 with a range of 0.07 - 0.92 (Fig. 6), or 0.36
with a range 0.12 - 1.58 when we compensate for density-dependence (Fig. 6). Our
sites are likely not network persistent, as our best estimates and most of the values we
402 see in our runs with uncertainty are below one, but network persistence is possible, as
our range of estimates does exceed one when we compensate for density-dependence.
We see that most of the connectivity occurs among the sites in the northern part of
405 our sample area, from Palanas to Caridad Cemetery, and at the southern part of our
sample area from Tomakin Dako to Sitio Baybayon (Fig. 6b, d), where the largest
sites are.

408 Based on our estimates of LRP, LRP_{local} , SP, and NP, it is possible but not likely
that our set of sites is able to persist in isolation as a closed system. With our
site configuration and dispersal kernel estimate, we would need a value of LRP of
411 3.99 (an egg-recruit survival of 0.0038 with our estimated value of LEP or a value
of LEP of 5095 or 2975 with our estimated egg-recruit survival compensating and
not compensating for density-dependence, respectively), to have a best estimate of

⁴¹⁴ $\lambda_c = 1$ and network persistence.

Discussion

We do not see strong evidence for persistence in our metric estimates. We see no
⁴¹⁷ evidence for self-persistence where an individual site could persist alone and weak
evidence for network persistence; it is possible at the upper end of our range of esti-
mates with uncertainty but not suggested by most of the range or our best estimates
⁴²⁰ (Fig. 6). The abundances through time at our sites do not show a clear directional
change, however, suggesting that the population at our sites is relatively constant
but relies on input of recruits from outside sites to persist. The portion of coastline
⁴²³ we sampled is likely a sink portion of a larger metapopulation.

For our sites to be able to persist as a network on their own, the number of
surviving recruits produced by an average recruit - LRP - would likely need to be
⁴²⁶ higher. With our estimated connectivity, LRP would need to be at least 3.99 to
see network persistence among our sites, which is within the top of our range of
uncertainty but about 3-5 times higher than our best estimates, without and with
⁴²⁹ density-dependence compensation. Our best estimate of LRP when we compen-
sate for density-dependence is greater than one, so higher connectivity and retention
of offspring among our sites could lead to network persistence, but almost all sur-
⁴³² viving offspring would need to be retained. At our best estimate without density-
dependence compensation, however, LRP is less than one - the average recruit only
produces 0.83 of a surviving recruit of the same stage - so no amount of increased
⁴³⁵ retention or connectivity, even retaining all of the recruits produced from our sites,

would lead to network persistence. Similarly, if other surrounding patch populations had a similar LRP, increasing the area of the network to include them would also not
438 achieve network persistence. If nearby sites have higher egg production or survival to recruit, however, it might not take much of an increase in area considered to create a persistence network. Nearby reef sites such as Cuatro Islas have higher quality
441 habitat and could be contributing recruits to our sites.

We do not find clear evidence for network persistence for our sites despite estimates of the mean dispersal distance of *A. clarkii* from previous genetic work (11
444 km, Pinsky et al., 2010) and from our samples (8.25 km, with 95% confidence interval 7.41 to 9.36, Catalano et al., in prep) that are well within the 30 km span of our sites. Though the width of our sampling region is more than twice the mean
447 dispersal distance, which Lockwood et al. (2002) find sufficient for persistence of an isolated reserve, their estimate assumes continuous habitat within the reserve and our region is only about 20% habitat. For a habitat configuration more similar to
450 our system, habitat patches (reserves) spaced on a coastline with non-habitat in between, they find that either 40% of the coastline needs to be preserved or a minimum patch size must be 1.25 times the mean dispersal distance to ensure persistence. Our
453 largest site, Haina, is only about 0.8 km wide, about 10 times less than the mean dispersal distance, so it is possible we do not have enough habitat in our region for network persistence, exacerbated by our 4 largest sites being at the edges of our
456 area and sending half of their recruits away from our sites. Our low, and possibly below-replacement, estimate for LRP also suggests that lack of persistence in these sites is not due to excessive dispersal out of the area but due to low production and

459 survival of offspring. The reef health and habitat quality in our sites is generally
460 low, due anthropogenic effects such as pollution and silt from a nearby gravel mine,
461 and habitat disturbance due to storms. Our sites are in an area that was hit in 2013
462 by Typhoon Haiyan, one of the strongest typhoons ever to make landfall, which de-
463 stroyed much of the reef habitat in some of our northern sampling areas. This recent
464 disturbance and generally low habitat quality could contribute to low production of
465 surviving recruits in our sites (seen in other populations with low habitat quality,
e.g. Hayashi et al., 2019) necessitating subsidization by outside populations.

We see considerable uncertainty in our estimate of persistence metrics depending
466 on the particular input values we use (Figs. 5, B.10). Our highest estimate for LRP
467 is about 24 times more than our lowest estimate and our highest NP estimate is
about 22 larger than our lowest, spanning the range between network persistence
471 for our set of sites to far from it. Measuring demographic and dispersal parameters
in the field is challenging; in the face of limited and imperfect data, characterizing
474 uncertainty and propagating it from our estimates of demographic and dispersal
inputs through to our estimates of persistence metrics is important to contextualize
our results. In our study, uncertainty in egg-recruit survival (a commonly challenging
parameter to estimate, e.g. Johnson et al., 2018; Hameed et al., 2016), partially driven
477 by uncertainty in how likely we are to capture recruits during sampling (Figs. B.9,
??), has a large effect on whether or not we think our populations are persistent.
For a marine metapopulation, our system is relatively uncomplicated and yet still
480 hard in which to concretely ascertain persistence. As we accumulate more empirical
assessments of metapopulations to compare to our expectations from theory and

models, we will have to think carefully about how to handle uncertainty as we move
483 to tackling larger and more complicated systems.

Persistence criteria, such as those detailed in Hastings and Botsford (2006a) and
Burgess et al. (2014), ask whether a population at low abundance can grow and
486 recover rather than going extinct. Density-dependence is often ignored at low abundances (e.g. Caswell, 2001; Hastings and Botsford, 2006b) so is not explicitly considered in persistence metrics. In real populations, however, it can be challenging
489 to estimate density-independent demographic rates, as density-dependence is occurring in the population as it is sampled. In *A. clarkii*, density-dependence is likely most important in early life stages, as for many fish species, but could play an im-
492 portant role throughout the life history due to the social hierarchies in colonies of clownfish (e.g. Buston and Elith, 2011). In other species of clownfish, individuals on the same anemone maintain strict size spacing, restricting their food intake and
495 growth to avoid encroaching on the position of another fish and being attacked or evicted (seen in *A. percula*, Buston, 2003a,b). This suggests that while fish are in the pre-reproductive queue, density-dependence may lower growth rates compared to
498 the growth of fish alone on an anemone, as would be the case in a population at low abundance. We attempt to account for the primary effect of density-dependence on our estimate of egg-recruit survival but other estimates, particularly growth and sur-
501 vival, would also likely be higher in the absence of density-dependence and increase LRP.

Our estimates of persistence metrics suggest that it is possible but not likely that
504 the region of sites we sample persist as a network without outside input, despite

covering an area more than twice the estimated mean dispersal distance for our focal species. Our estimate of LRP near the threshold of one required for replacement
507 (slightly < 1 when we do not compensate for density-dependence, slightly > 1 when we do), suggests that dispersal is not likely the primary reason our sites do not persist as a network. If density-dependence is strongly present in our data such that our
510 compensated estimate is the best, then our sites could persist if there were no losses to dispersal. Otherwise, our sites do not produce enough offspring for replacement regardless of dispersal patterns, possibly due to worsening habitat quality. This is
513 a reminder that dispersal is only part of the persistence story for metapopulations; even areas that seem large enough to contain a persistent network based on dispersal distance will not be able to persist in isolation if they have low production and
516 survival of offspring. We do find recruits coming back to our region, and even to their natal site, but broader connectivity to more productive sites likely enables our sites to persist.

⁵¹⁹ **Figures**

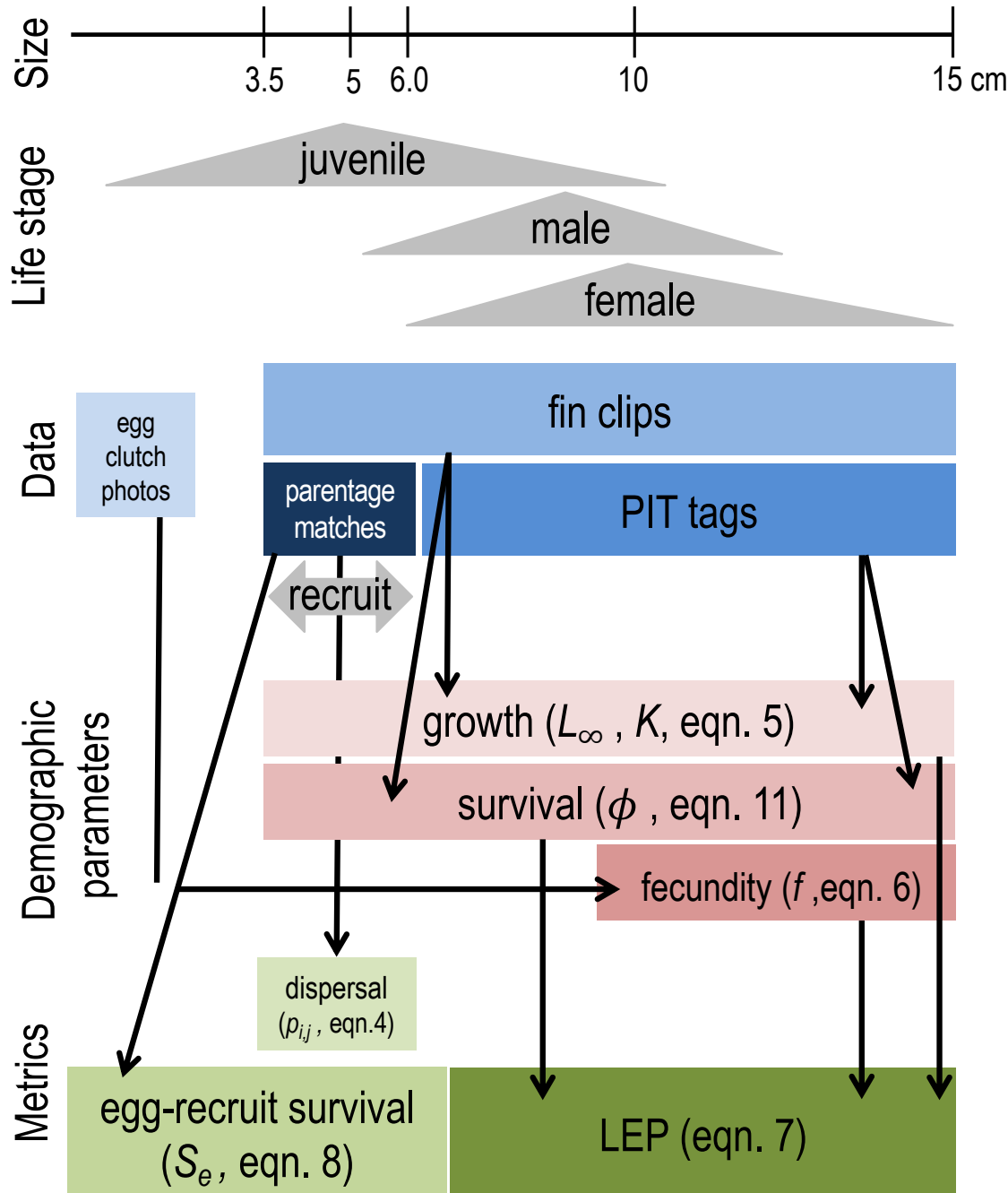


Figure 2: This schematic represents the data collected for fish at each life stage and how they match to the equations and metrics we estimate. We consider recruits to be offspring in their first year of settlement, represented by the 3.5-6.0 cm range.

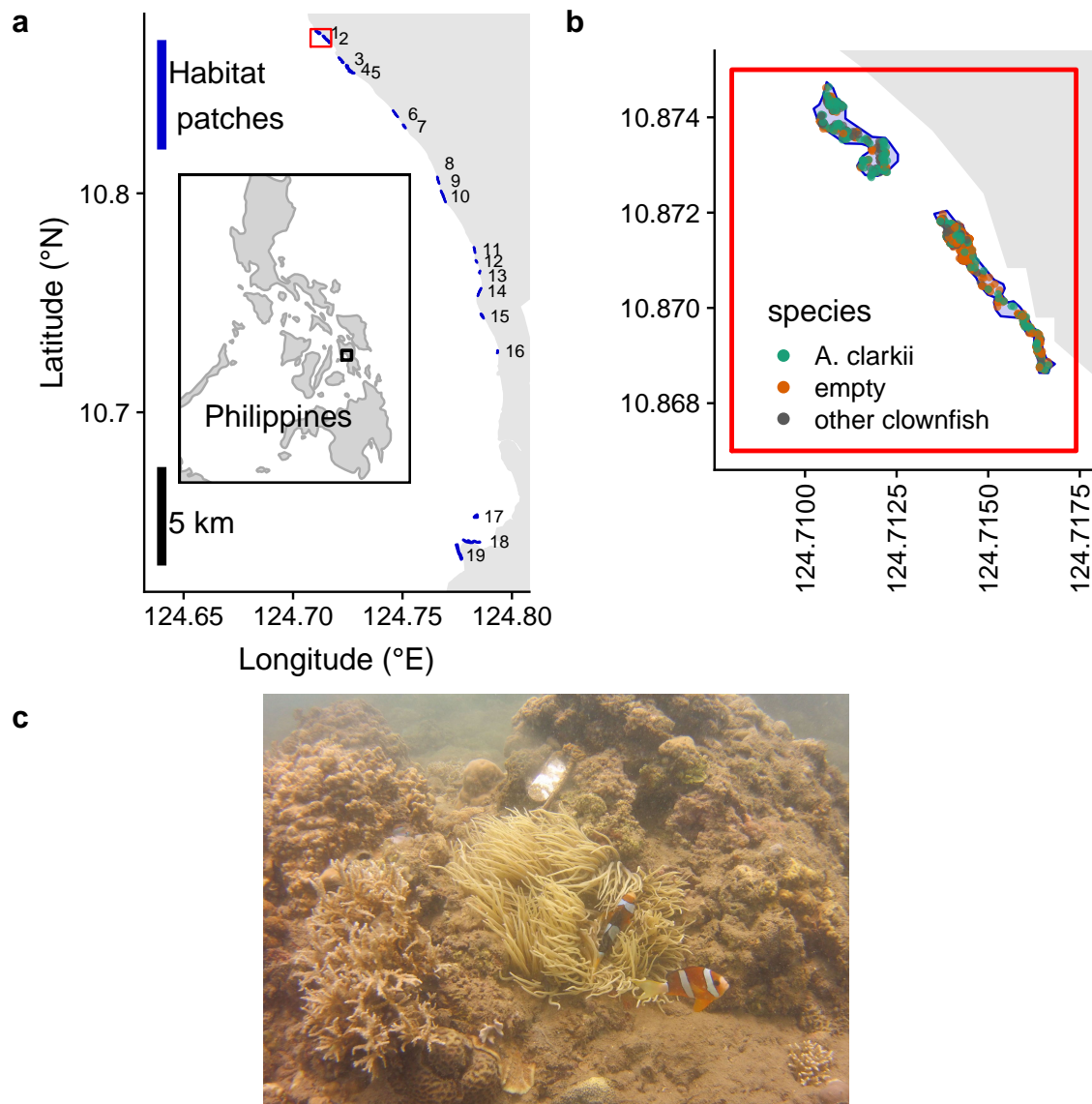


Figure 3: a) Map of the sites along the coast of Leyte in the Philippines. Patches are: 1) Palanas, 2) Wangag, 3), North Magbangon, 4) South Magbangon, 5) Cabatoan, 6) Caridad Cemetery, 7) Caridad Proper, 8) Hicop South, 9) Sitio Tugas, 10) Elementary School, 11) Sitio Lonas, 12) San Agustin, 13) Poroc San Flower, 14) Poroc Rose, 15) Visca, 16) Gabas, 17) Tomakin Dako, 18) Haina, and 19) Sitio Baybayon. b) Zoomed-in map of the two northern-most sites, Palanas and Wangag, to show anemone arrangement, with anemones occupied by *A. clarkii* (green), occupied by other clownfish species (orange), or unoccupied by clownfish (grey). c) An example anemone occupied by *A. clarkii* in a typical habitat at the sites. The metal anemone tag is visible just above the anemone on the rock.

29

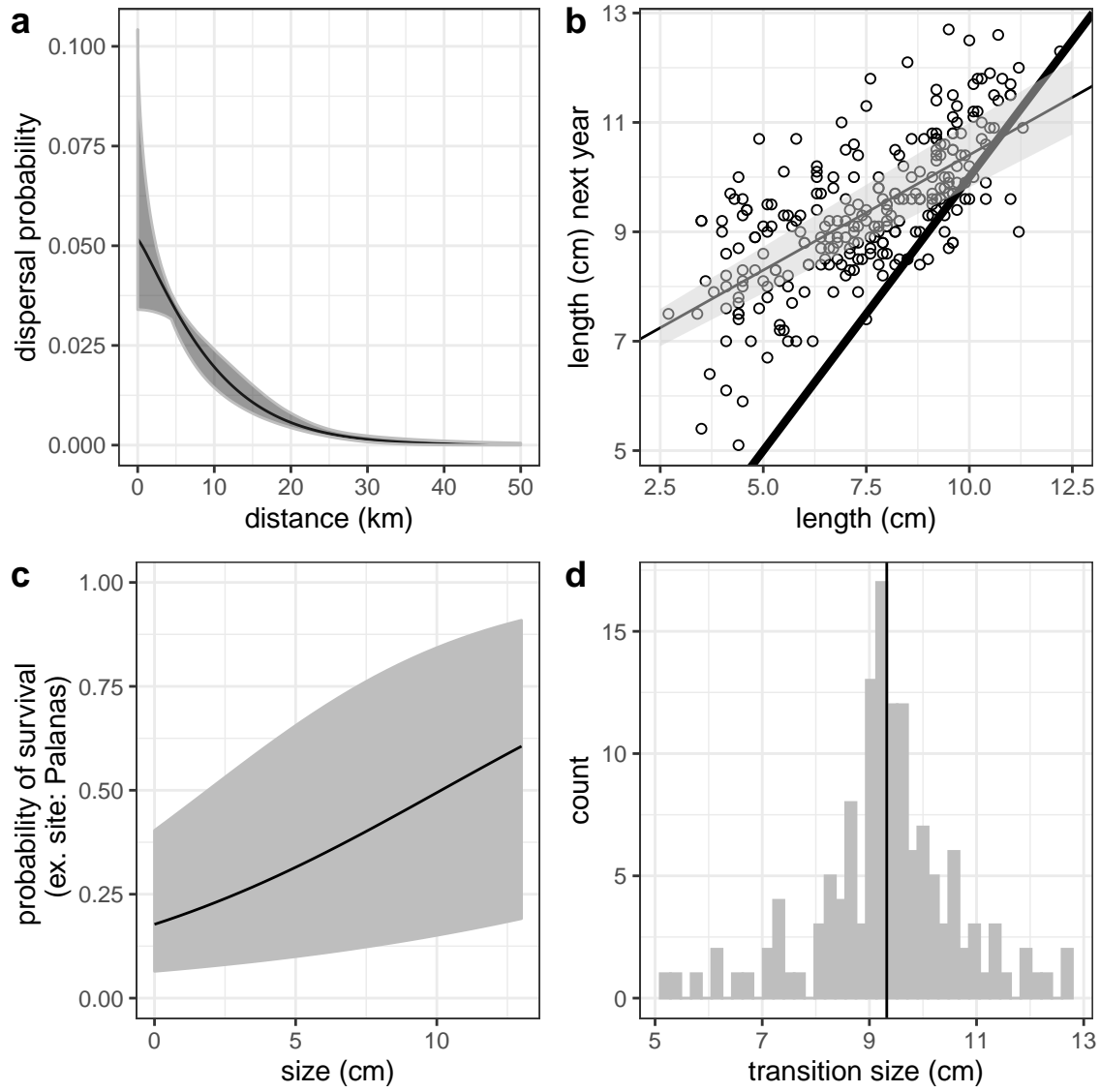


Figure 4: Best estimates (solid black line) and range included for uncertainty (gray) for dispersal (a), growth, including the 1:1 line in thick black (b), post-recruit annual survival at Palanas as an example site (c), and size at female transition (d) parameters.

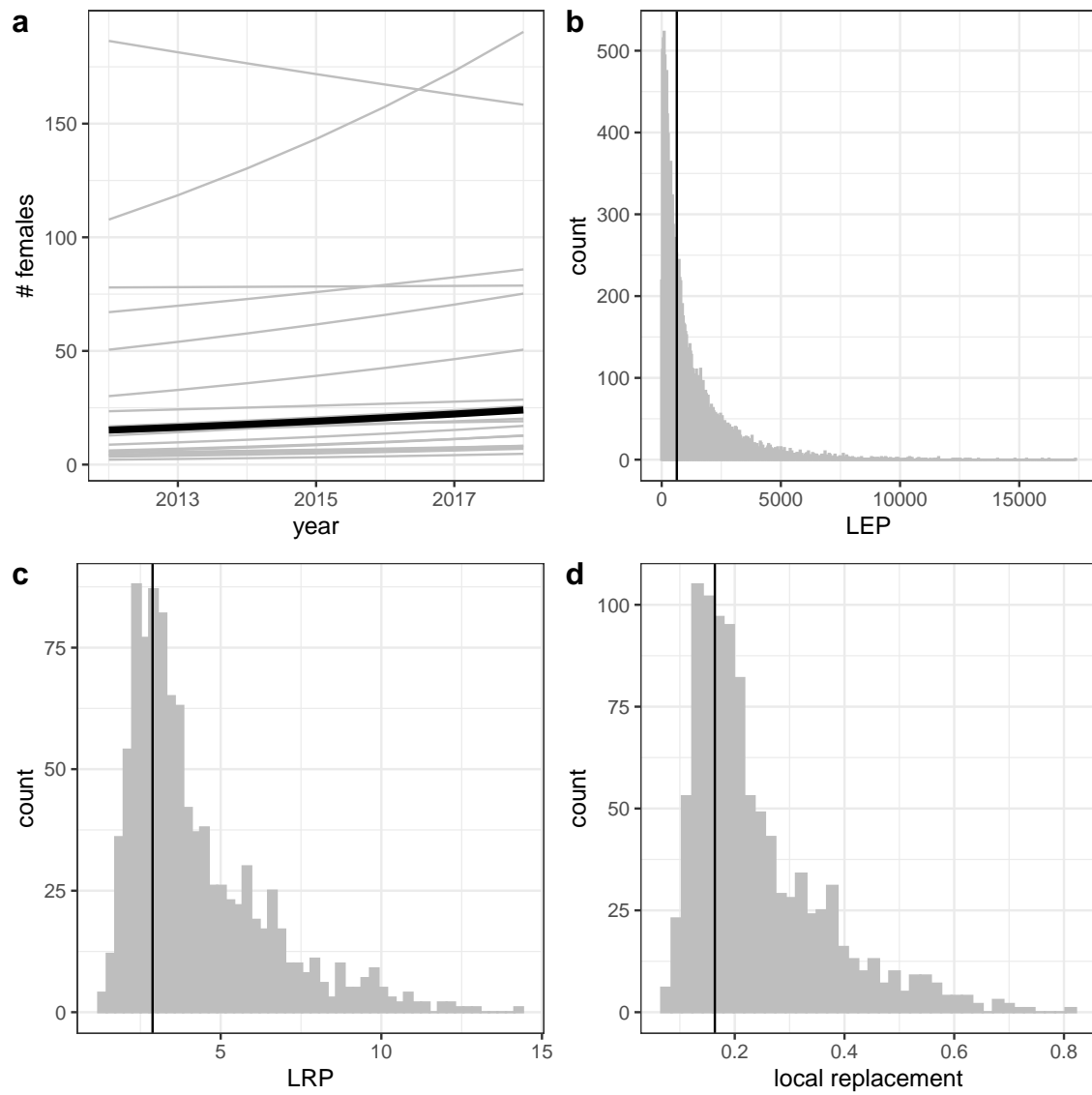


Figure 5: Estimates of a) estimated abundance of females at each individual site (grey lines) and for an average site (black line) across time b) individual site LEP for all sites, c) average LRP across sites, and d) local replacement, showing the best estimate (black solid line) and range of estimates considering uncertainty in the inputs. Estimates of LRP and local replacement include compensation for density-dependent mortality in early life stages.

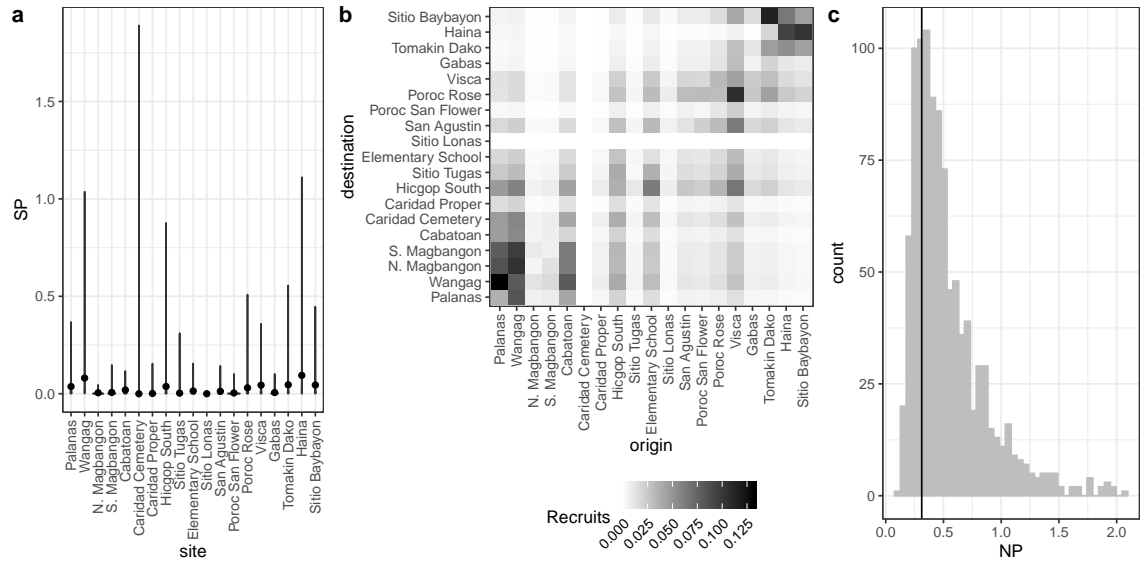


Figure 6: Values of self-persistence (a), realized connectivity among sites (b), and network persistence (c). All estimates include compensation for density-dependence in early life stages in our data. For self-persistence (a) and network persistence (c), the best estimate is shown with in black (point for (a), line for (c)) and the range of estimates considering uncertainty is shown in grey.

Appendix

Summary of parameters

| Parameter | Description | Best estimate | Range in uncertainty runs | Notes |
|------------|---|---------------|---------------------------|--|
| k_d | scale parameter in dispersal kernel | -2.11 | -2.36 to -1.96 | estimated using methods in Bode et al. (2018) in Catalano et al. (in prep) |
| θ | shape parameter in dispersal kernel | 1 | NA | estimated using methods in Bode et al. (2018) in Catalano et al. (in prep) |
| L_∞ | average asymptotic size in von Bertalanffy growth curve | 10.70 cm | 10.50 to 10.90 cm | |

| | | | | |
|----------|--|--------|----------------------------|---|
| K | growth coefficient in von Bertalanffy growth curve | 0.864 | 0.785 to 0.944 | |
| b_ϕ | intercept for adult survival | -1.82 | ± 0.231 standard error | on a log-odds scale |
| b_a | size effect for adult survival | 0.169 | ± 0.028 standard error | on a log-odds scale |
| b_{pr} | intercept for recapture probability from mark-recapture analysis | 2.10 | ± 0.849 standard error | on a log-odds scale, not used in persistence estimates |
| b_1 | size effect for recapture | -0.161 | ± 0.088 standard error | on a log-odds scale, not used in persistence estimates |
| b_2 | distance effect for recapture | -0.196 | ± 0.023 standard error | on a log-odds scale, not used in persistence estimates |

| | | | | |
|-----------------------------|---|---|--------------|--|
| size _{recruit} | size (cm) of recruited offspring | mean of size of offspring in parentage analysis = 4.37 cm | 3.5 - 6.0 cm | drawn from uniform distribution across range |
| size _{recruit, sd} | standard deviation of size of a recruit | 0.1 | | used in discretization of IPM for LEP |
| size _{sd} | standard deviation distribution of sizes of a fish in the next year | 1.45 | | used in discretization of IPM for LEP, estimated from range of sizes for fish starting at 7.4-7.6 cm and recaptured a year later |
| b_e | coefficient for eyed eggs | -0.608 | | Yawdoszyn et al. (in prep) |
| b_l | size effect in eggs-per-clutch relationship | 2.39 | | Yawdoszyn et al. (in prep) |
| b | intercept in eggs-per-clutch relationship | 1.17 | | Yawdoszyn et al. (in prep) |

| | | | | |
|-------|---|--------|--|---------------------------------|
| c_e | egg clutches per year | 11.9 | | Holtswarth et al. (2017) |
| L_f | size at transition to female | 9.32cm | 5.2 - 12.7cm | drawn from distribution in data |
| P_h | proportion of sites sampled cumulatively across time | 0.41 | | details in A.1 |
| P_d | proportion of dispersal kernel area from each site covered by our sampling region | 0.57 | | details in A.2 |
| P_c | probability of capturing a fish | 0.56 | drawn from beta distribution with parameters $\alpha_{P_c} = 1.44$ and $\beta_{P_c} = 1.13$ | details in A.2 |

| | | | | |
|-------|--|------|--|---------------------|
| P_s | proportion of our sampling region that is habitat | 0.20 | | details in A.2.0.1 |
| DD | proportion of habitat that would be available without density-dependence at settlement | 1.71 | | |
| p_U | proportion of anemones unoccupied by clownfish | 0.53 | | used to estimate DD |
| p_A | proportion of anemones occupied by <i>A. clarkii</i> | 0.38 | | used to estimate DD |
| L_s | minimum size in LEP IPM | 0 | | eqn. 7 |

| | | | | |
|-------|----------------------------|----|--|--------|
| U_s | maximum size in LEP IPM | 15 | | eqn. 7 |
|-------|----------------------------|----|--|--------|

Table A1

⁵²² **A Method details**

A.1 Proportion of habitat sampled

We used tagged anemones to estimate the proportion of habitat sampled at each site in each year ($P_{h_{i,t}}$). We tagged each anemone that is home to *A. clarkii*, with a metal tag, which is relatively permanent and easy to re-sight (the anemone tag is visible above the anemone in Fig. 3c), so we consider the total number of metal tags at each site to be the total number of anemones that are habitat. We divide the number of tagged anemones visited each sampling year by the total number of metal tags at that site to get the proportion of habitat sampled. We use proportion of anemones rather than proportion of total site area because anemones, and therefore habitat quality, are unevenly distributed across the site; areas we did not visit are likely to have a lower density of anemones than the areas we did sample.

⁵³⁴ For scaling the number of tagged recruited offspring to account for areas of our sites we did not sample, we use the overall proportion habitat sampled across all sites and sampling years (P_h). We sum the metal-tagged anemones we visited across all sites and years to get the total number of metal-tagged anemones we visited while sampling. We then divide that by the number of anemones we could have sampled,

| Site | # Total anems | % Habitat surveyed | | | | | | |
|-------------------|---------------|--------------------|------|------|------|------|------|------|
| | | 2012 | 2013 | 2014 | 2015 | 2016 | 2017 | 2018 |
| Cabatoan | 26 | 42 | 58 | 58 | 65 | 73 | 0 | 62 |
| Caridad Cemetery | 4 | 0 | 75 | 50 | 0 | 50 | 50 | 50 |
| Elementary School | 8 | 0 | 100 | 38 | 88 | 88 | 88 | 100 |
| Gabas | 9 | 0 | 0 | 0 | 44 | 44 | 67 | 0 |
| Haina | 104 | 0 | 6 | 13 | 13 | 10 | 56 | 80 |
| Hicgop South | 18 | 0 | 67 | 22 | 28 | 56 | 83 | 78 |
| N. Magbangon | 105 | 5 | 12 | 40 | 63 | 63 | 0 | 5 |
| S. Magbangon | 34 | 41 | 56 | 32 | 0 | 65 | 0 | 71 |
| Palanas | 137 | 29 | 58 | 47 | 63 | 85 | 86 | 86 |
| Poroc Rose | 13 | 100 | 100 | 69 | 31 | 23 | 69 | 69 |
| Poroc San Flower | 11 | 100 | 82 | 73 | 73 | 55 | 82 | 64 |
| San Agustin | 17 | 94 | 65 | 71 | 65 | 100 | 82 | 76 |
| Sitio Baybaon | 260 | 0 | 14 | 30 | 33 | 30 | 41 | 80 |
| Tomakin Dako | 50 | 0 | 24 | 22 | 36 | 34 | 60 | 68 |
| Visca | 13 | 100 | 100 | 23 | 38 | 62 | 85 | 62 |
| Wangag | 296 | 18 | 32 | 42 | 34 | 26 | 49 | 68 |

Table A2: Table showing the percent of metal-tagged anemones surveyed at each site in each sampling year.

the sum of total metal-tagged anemones across all sites multiplied by the number of
 540 sampling years, to get the overall proportion habitat sampled across our sites and
 sampling years.

A.2 Probability of capturing a fish, from recapture dives

543 We use mark-recapture data from recapture dives done within a sampling season to
estimate the probability of capturing a fish. During some of the sampling years (XX),
portions of the sites were sampled again XX-XX weeks after the original sampling
dives. We assume there is no mortality of tagged fish between the original sampling
dives and the recapture dives because they are so close in time and that fish do not
change their behavior or response to divers, so therefore assume that the probability
549 of recapturing a fish is the same as the probability of capturing a fish on a sample dive.
For each recapture dive, we use GPS tracks of the divers to identify the anemones
covered in the recapture dive and the set of PIT-tagged fish encountered on those
552 anemones during the original sampling dives. We estimate the probability of capture
 P_c as the number of tagged fish caught during the capture dive m_2 divided by the
total number of fish caught on the recapture dive n_2 : $P_c = \frac{m_2}{n_2}$.

555 We use the mean P_c across all 14 recapture dives, covering XX sites in 3 sampling
seasons (2016, 2017, 2018), as our best estimate. Because there are so few recapture
dives compared to the number of times we calculate the metrics to show the range
558 of uncertainty, we represent the probability of capture as a distribution, rather than
pulling directly from the values calculated for each recapture dive. The distribution
of capture probabilities across the 14 dives is quite skewed so we represent it as a
561 beta distribution, using the mean μ_{P_c} and variance V_{P_c} of the set of 14 values to find
the appropriate α_{P_c} and β_{P_c} parameters, where

$$\alpha_{P_c} = \left(\frac{1 - \mu_{P_c}}{V_{P_c}} - \frac{1}{\mu_{P_c}} \right) \mu_{P_c}^2 \quad (\text{A.1})$$

$$\beta_{P_c} = \alpha_{\mu_{P_c}} \times \frac{1}{\mu_{P_c} - 1}. \quad (\text{A.2})$$

The mean of the individual capture probability values is $\mu_{P_c} = 0.56$, with variance
 564 $V_{P_c} = 0.069$, which gives beta distribution parameters $\alpha_{P_c} = 1.44$ and $\beta_{P_c} = 1.13$.
 We sample 1000 values from the beta distribution, then truncate the sample to only
 values larger than the lowest value of P_c estimated in an individual dive (0.20), to
 567 avoid extremely low values that are sometimes sampled but are unrealistically low.
 We then sample with replacement from the truncated set to get a vector of values
 the length of the number of runs.

570 Scaling up recruits

ADD SOME TEXT!

How could we have missed potential recruits originating from our sites?

- 1) Failed to catch recruit when sampling (P_c)
- 2) Missed sampling some habitat areas within our sites (P_h)
- 3) Recruit dispersed outside our study region (P_d)
- 4) Recruit dispersed to non-habitat within our region (P_s)
- 5) Recruit died due to density-dependent competition with other settlers (DD)

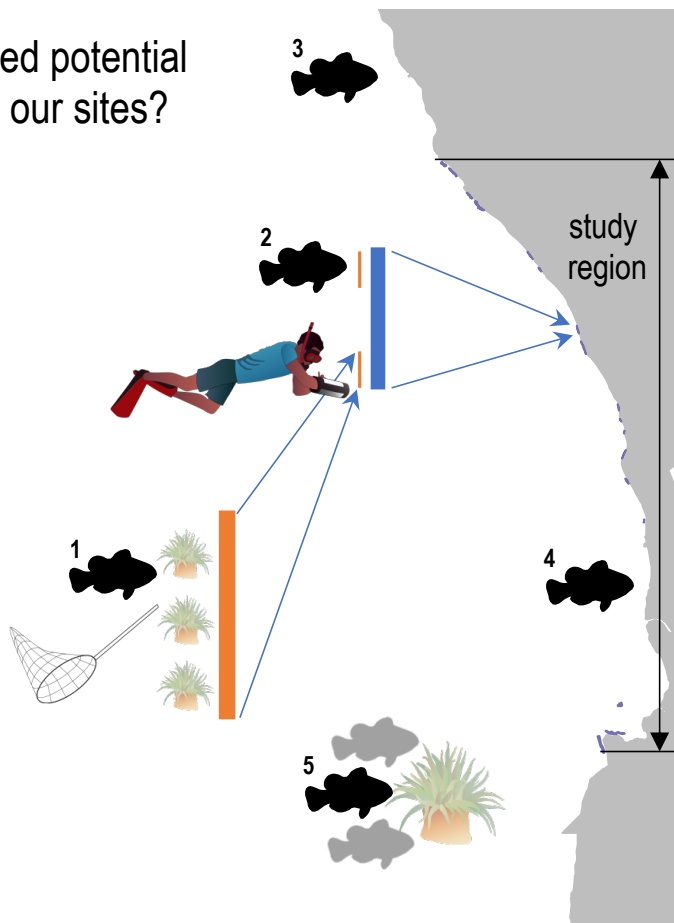


Figure A.1: Schematic of five ways we could have missed recruits while sampling and used to scale up our raw estimate of recruits from matched offspring.

Proportion of dispersal kernel area sampled

⁵⁷³ [Add in description of calculation and equation]

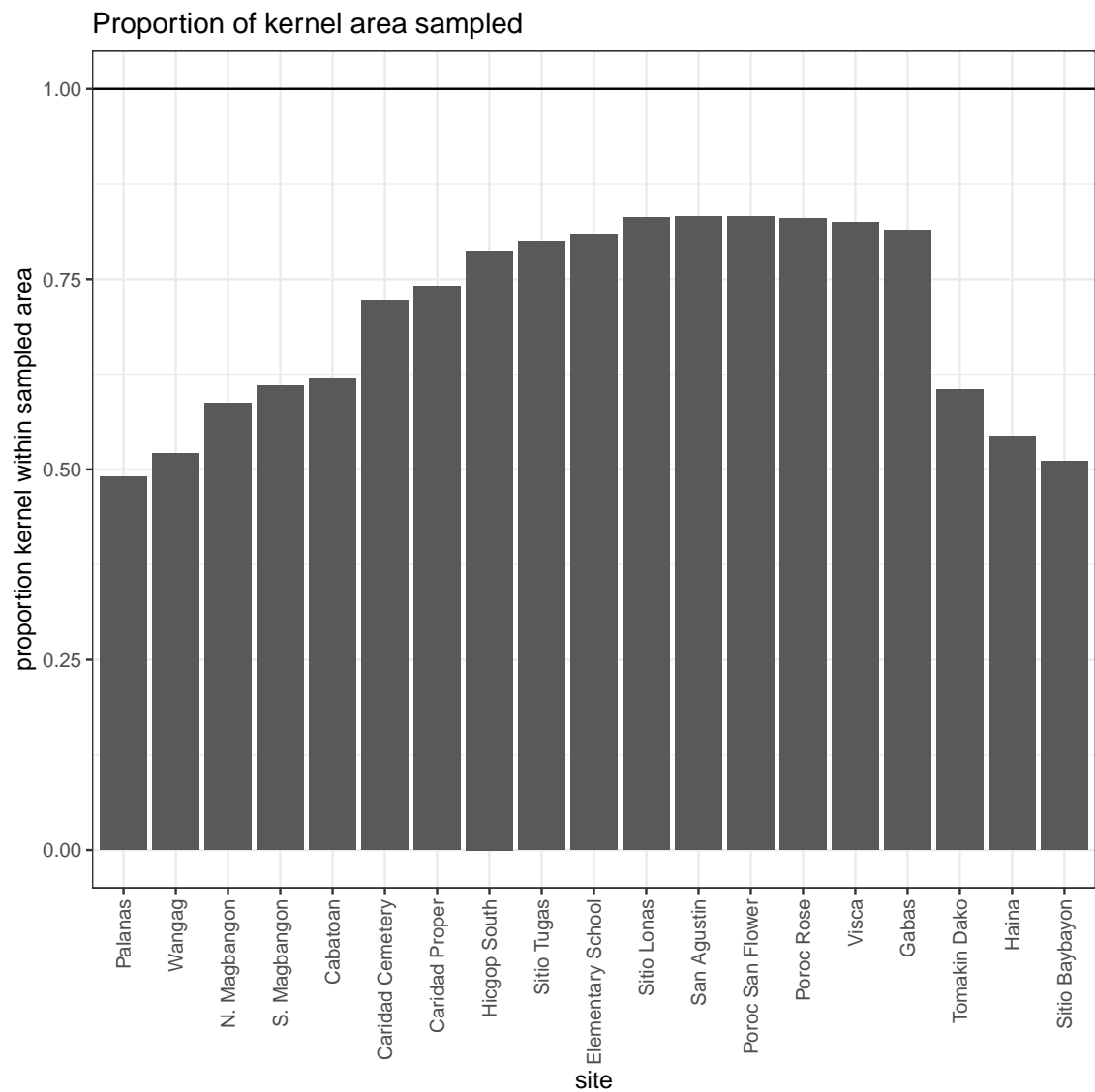


Figure A.2: Proportion of the dispersal kernel area from the center of each site covered by our sampling.

A.2.0.1 Proportion habitat in sampling area

We assume that larvae are unable to navigate to habitat if they attempt to settle
576 on an unsuitable patch, though clownfish larvae do likely have some ability both to
sense habitat (CITATIONS) and move toward it (CITATIONS)). To avoid counting
mortality due to settling on non-habitat twice - once in scaling up our matched
579 recruits, which only includes those who settled on habitat, and once in integrating
the dispersal kernel, we scale our estimate of total surviving recruits from our patches
by the proportion of our sampling region that is habitat (P_s). We find P_s by summing
582 the lengths of all of our sites, which run approximately north-south, and dividing
that by the total distance north-south of our sampling region, giving $P_s = 0.20$.

| Model | Model description | AICc | dAICc |
|-----------------------------|--|----------|-----------|
| $\phi \sim S, p \sim S + D$ | survival size, recapture size+distance | 3348.861 | 0 |
| $\phi \sim S, p \sim D$ | survival size, recapture distance | 3359.998 | -11.1371 |
| $\phi, p \sim D$ | survival constant, recapture distance | 3383.175 | 34.3141 |
| $\phi, p \sim S + D$ | survival constant, recapture size+distance | 3384.959 | 36.0981 |
| $\phi \sim t, p$ | survival time, recapture constant | 3408.342 | 59.4816 |
| $\phi \sim i, p$ | survival site, recapture constant | 3440.842 | 91.98112 |
| $\phi \sim i, p \sim S + D$ | survival site, recapture size+distance | 3440.842 | 91.98112 |
| $\phi, p \sim t$ | survival constant, recapture time | 3453.609 | 104.74839 |
| $\phi \sim S, p \sim S$ | survival size, recapture size | 3527.710 | 178.84940 |
| ϕ, p | survival constant, recapture constant | 3570.908 | 222.04690 |

Table A3

A.3 Full set of MARK models

- 585 We consider the following set of models in MARK for survival (ϕ) and recapture (p) probability, including effects of size (S), minimum distance from diver to anemone during surveys (D), time (t), and site (i) (Table A3):
- 588 The best model includes both site and size in survival

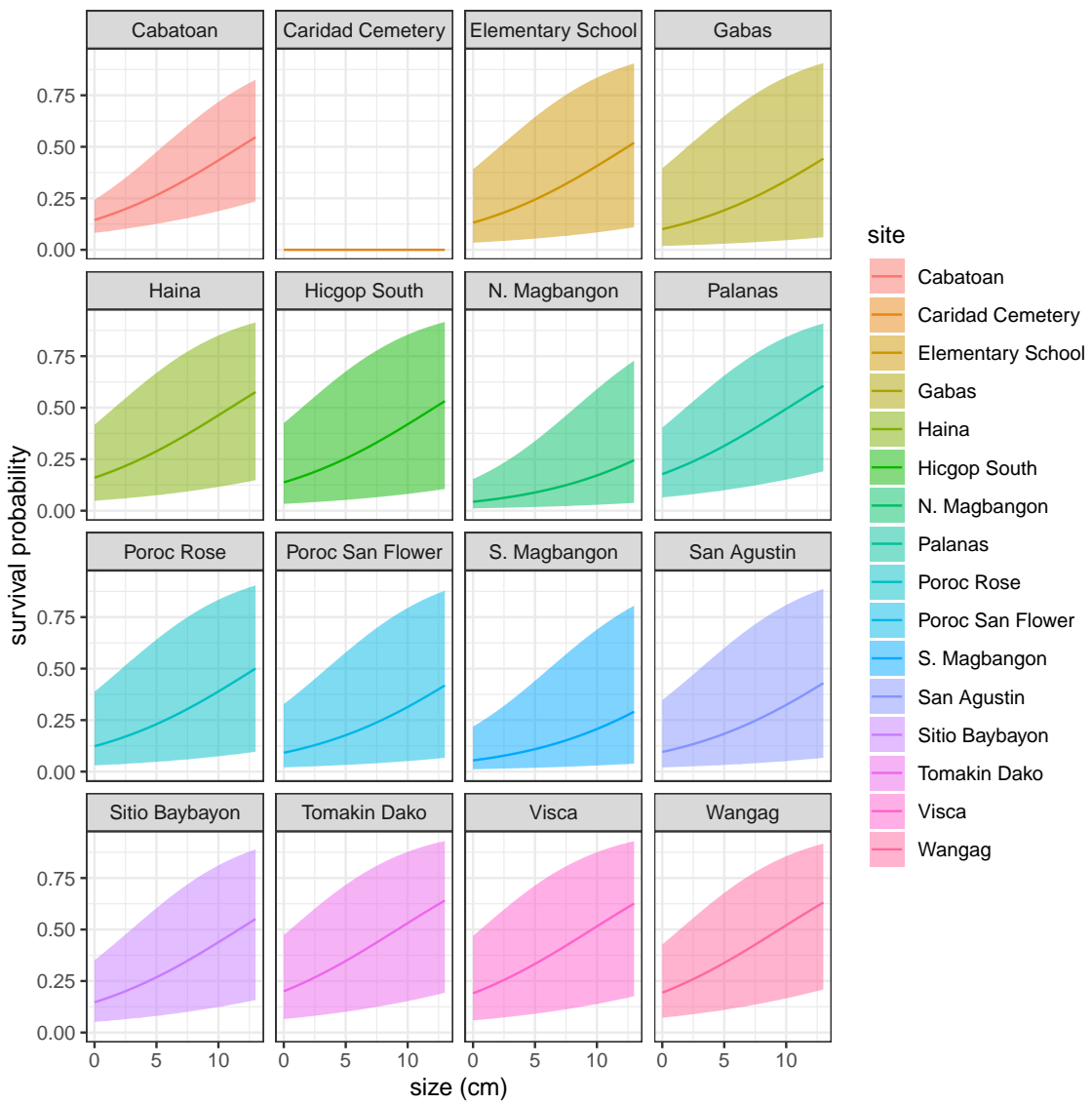


Figure A.3: Annual survival by size at each site.

A.3.0.1 Recapture model

The best model for log-odds recapture probability, accompanying the survival model
⁵⁹¹ in eqn. 11, has a size effect ($b_1 = -1.816 \pm 0.080$ SE, Fig. A.4a) and a negative

effect of diver distance from the anemone ($b_2 = -0.171 \pm 0.021$ SE, Fig. A.4b), with intercept $b_{pr} = 17.93 \pm 0.858$ SE:

$$\log\left(\frac{p_r}{1 - p_r}\right) = b_{pr} + b_1 \text{size} + b_2 d. \quad (\text{A.3})$$

- 594 The negative effect of both size and distance suggest that divers are less likely to recapture larger fish and those at anemones far from areas sampled.

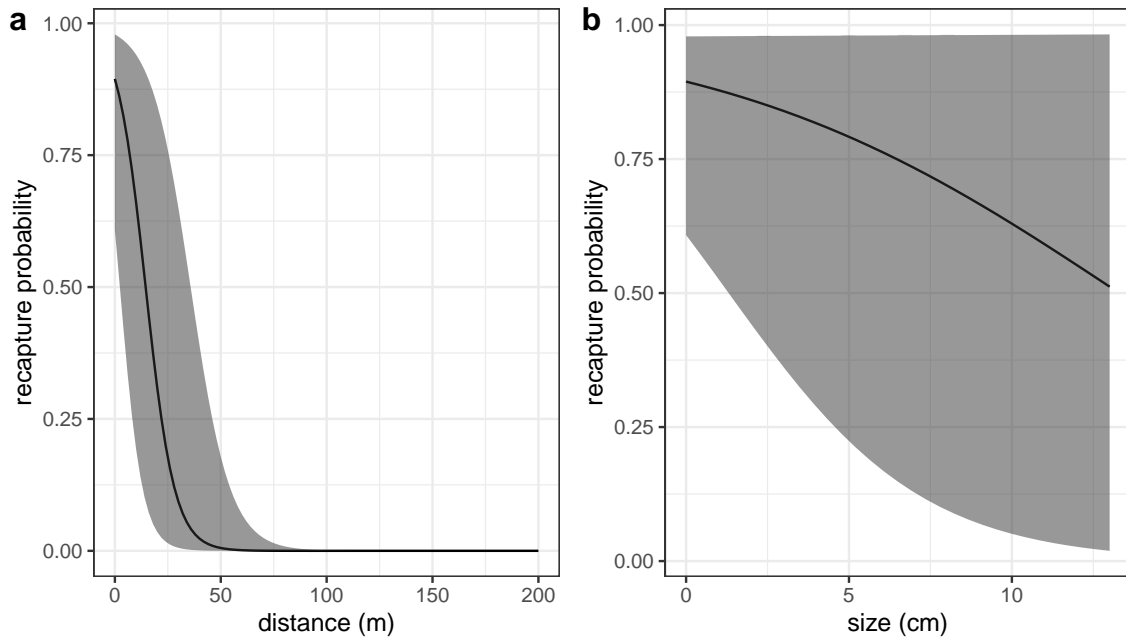


Figure A.4: Effects of a) minimum distance between divers and the anemone where the fish was first caught and b) fish size on the probability the fish will be recaptured, estimated along with survival in a mark-recapture analysis. Size has a slightly negative effect on the probability of recapture - larger fish are stronger swimmers and more likely to flee the anemone when divers approach, but with high uncertainty at larger sizes. Distance also has a negative effect on recapture, as fish tend to stay close to their anemones and are not likely to be recaptured if divers do not get close to their anemone.

B Result details and sensitivity

597 Abundance trends by site

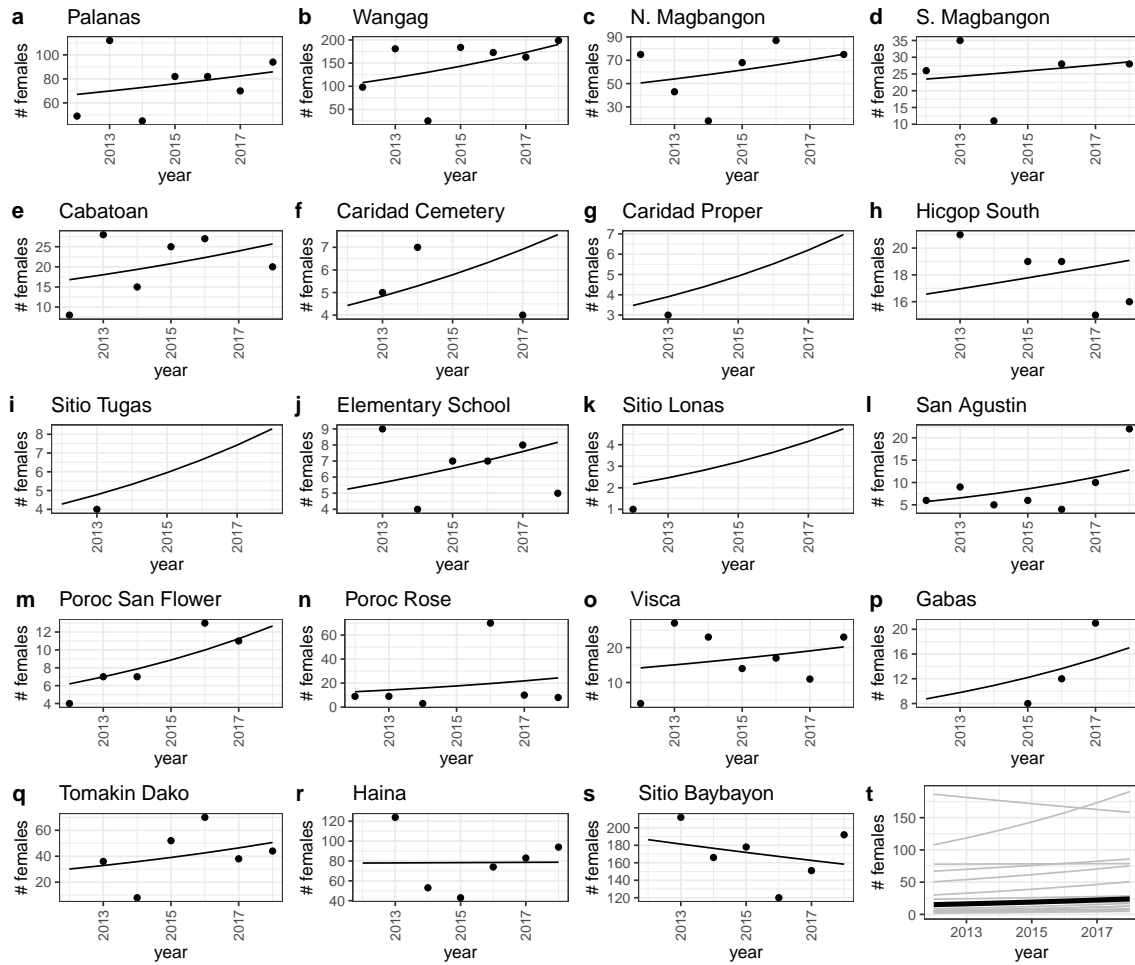


Figure B.1: Scaled estimates of females and abundance trends by site.

Compensating for density dependence

TALK ABOUT HOW DENSITY DEPENDENCE AFFECTS OUR RESULTS, CITE

600 SECTION OR EQUATION WHERE WE COMPENSATE FOR IT

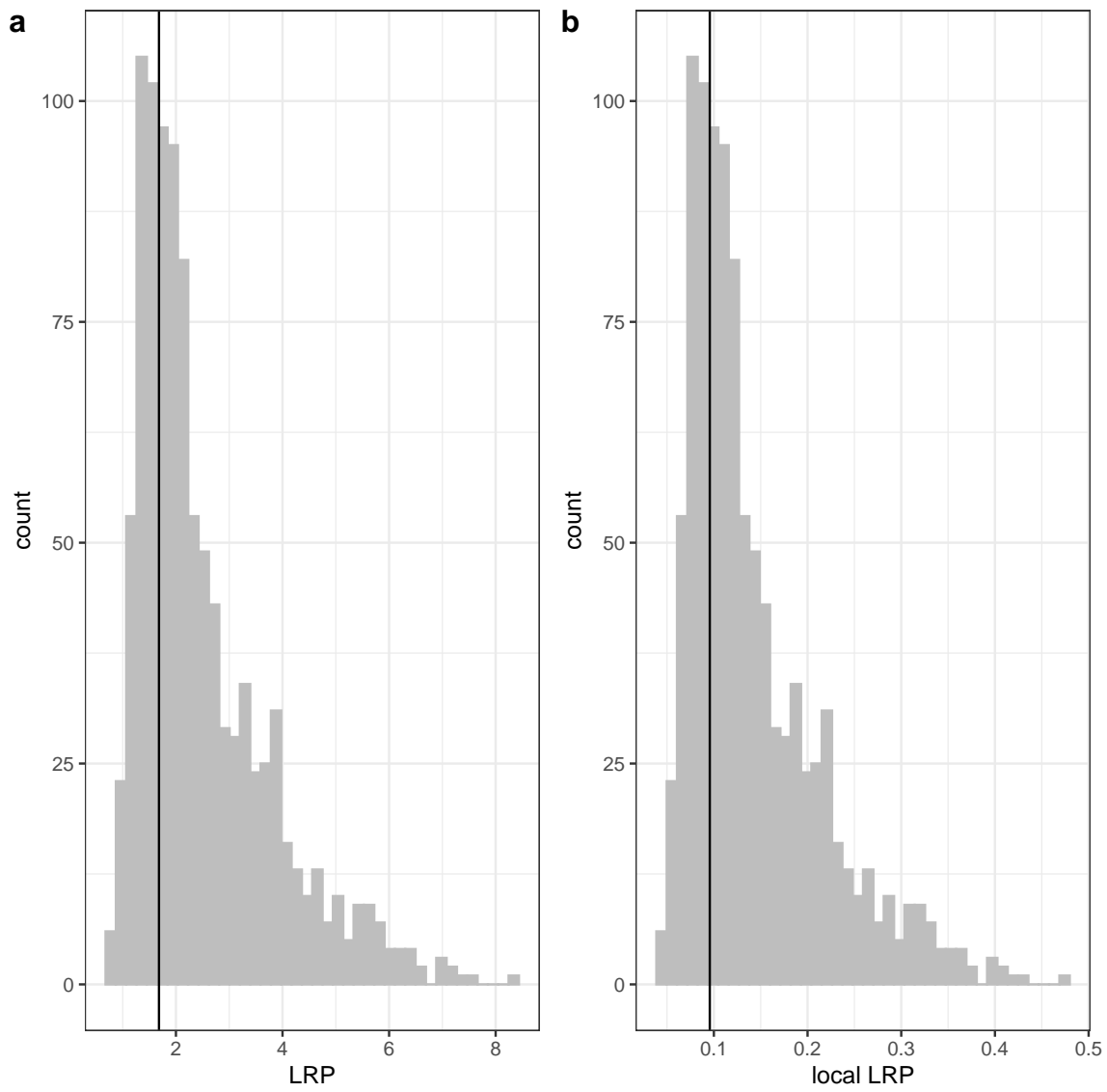


Figure B.2: Estimates of a) LRP, and b) local replacement without compensating for density dependence in early life stages in our data, showing the best estimate (black solid line) and range of estimates considering uncertainty in the inputs. These estimates compare to those in 5c,d, where we attempt to compensate for additional mortality in early life due to density dependence.

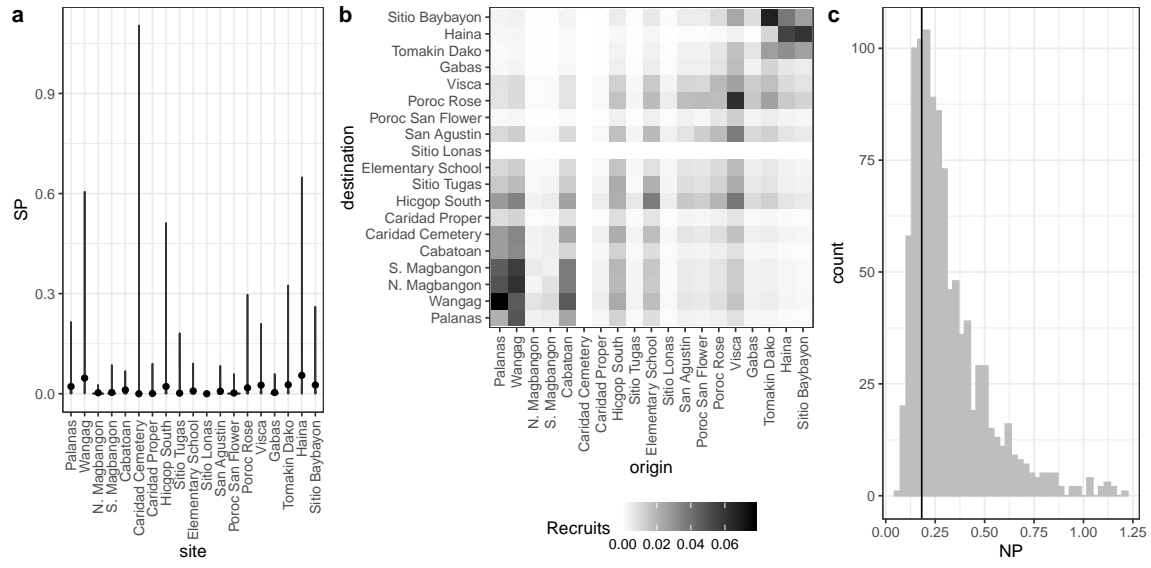


Figure B.3: Values of self-persistence (a), realized connectivity among sites (b), and network persistence (c) without compensation for density-dependence in early life stages in our data. For self-persistence (a) and network persistence (c), the best estimate is shown with in black (point for (a), line for (c)) and the range of estimates considering uncertainty is shown in grey. These estimates compare to those in 6 where we attempt to compensate for density dependence in early life stages.

LEP and LRP by site

WRITE SOME TEXT!

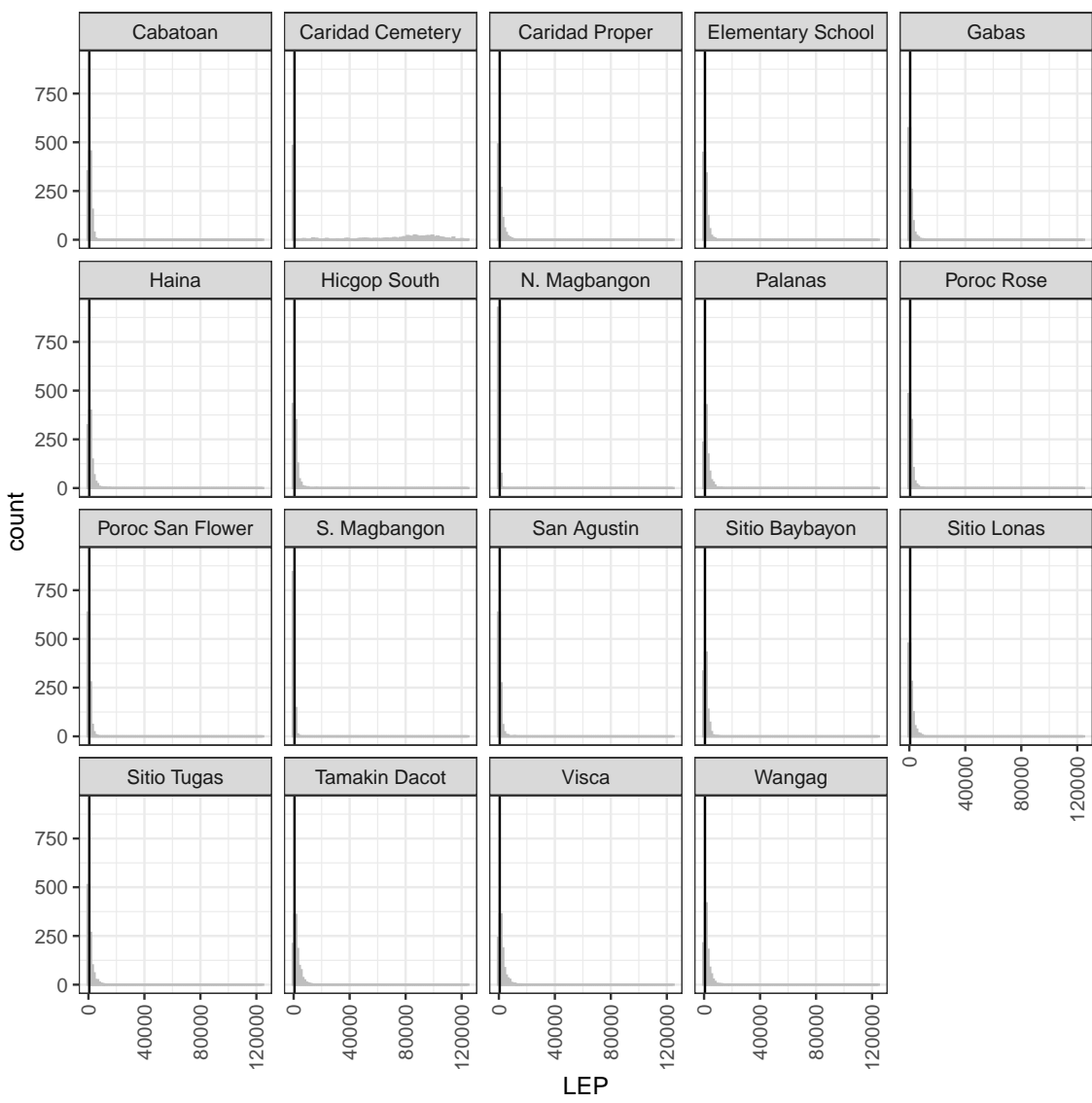


Figure B.4: Write a caption.

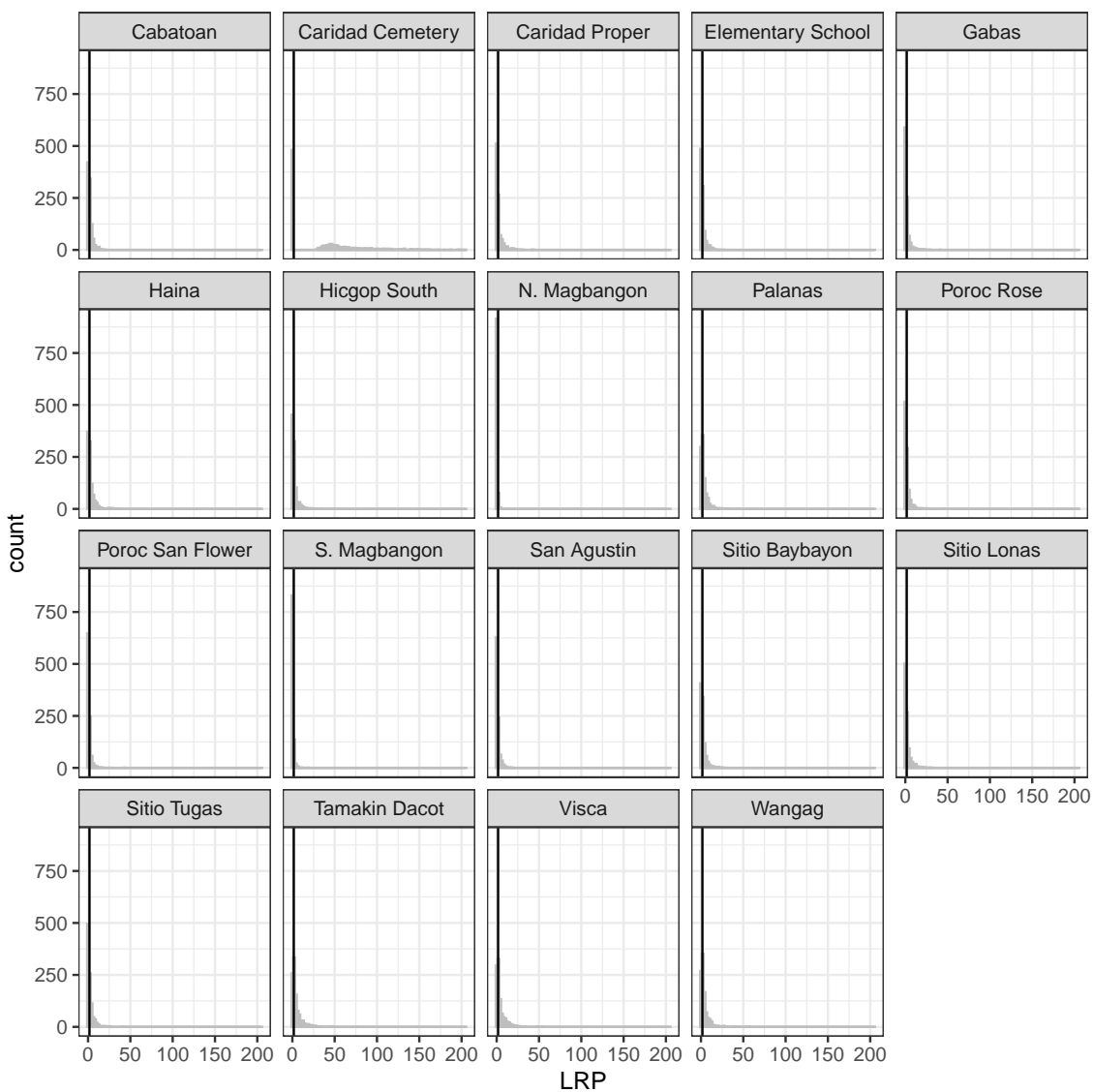


Figure B.5: Write a caption.

⁶⁰³ B.1 Sensitivity to parameters

EXPLAIN THAT THESE ARE THE REST OF THE PARAMETERS, NOT SHOWN
IN THE MAIN TEXT

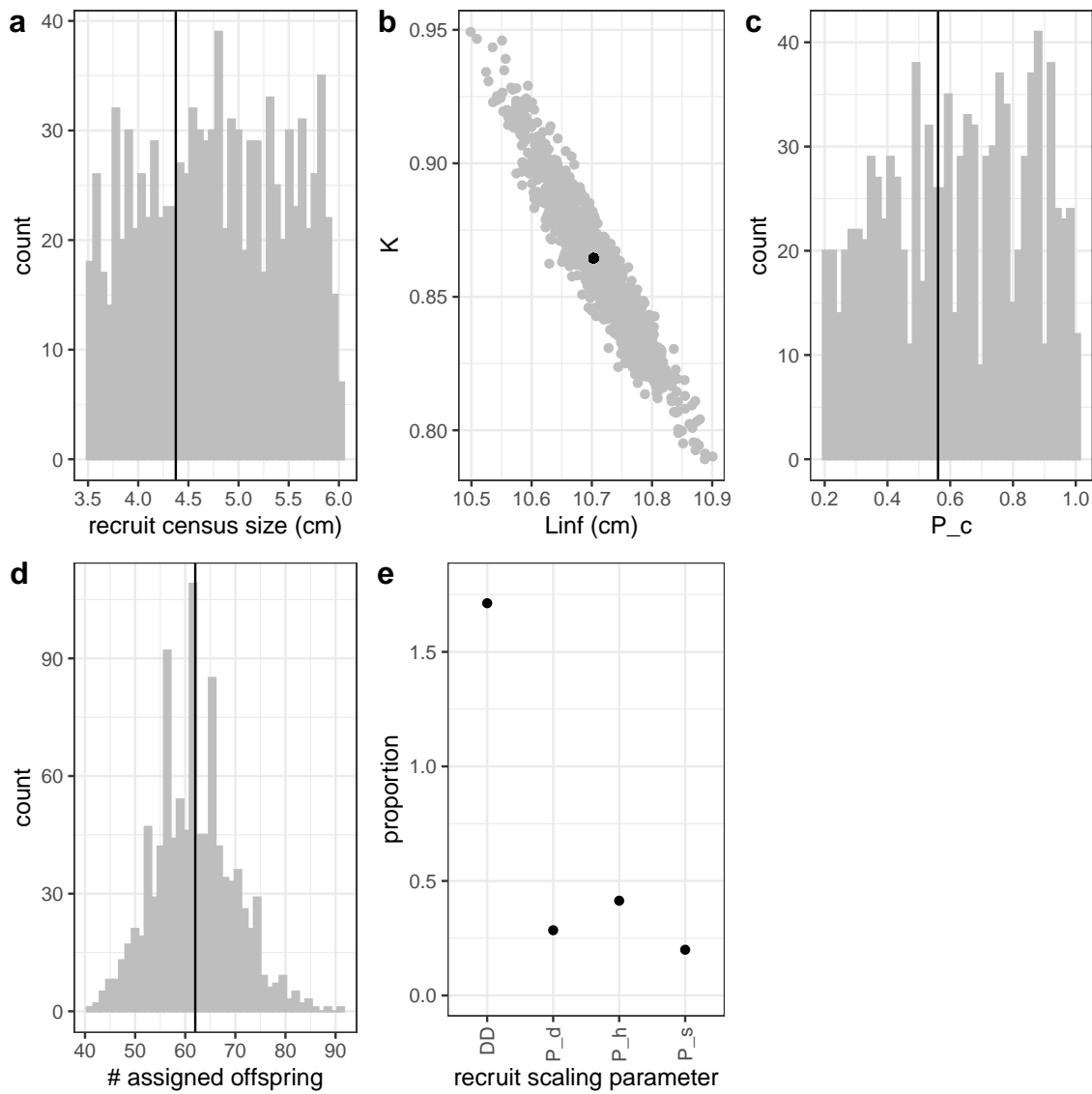


Figure B.6: Range of parameter inputs for uncertainty runs with all uncertainty included, where the black line or point is the value used for the best estimate: a) $\text{size}_{\text{recruit}}$, the census size at which fish are considered to have recruited after egg-recruit survival occurs; b) the parameters L_∞ and K of the von Bertalanffy growth model; c) P_c , the probability of capturing a fish; d) number of offspring assigned back to parents in the parentage analysis; e) factors that scale the number of estimated recruits from our site based on density-dependence in settler success (DD), proportion of the dispersal kernel captured by our sampling region (P_d), the cumulative proportion of our sites we sampled over time (P_h), and the proportion of our sampling area that is habitat (P_s). 54

606 **B.2 Effects of different types of uncertainty on metrics**

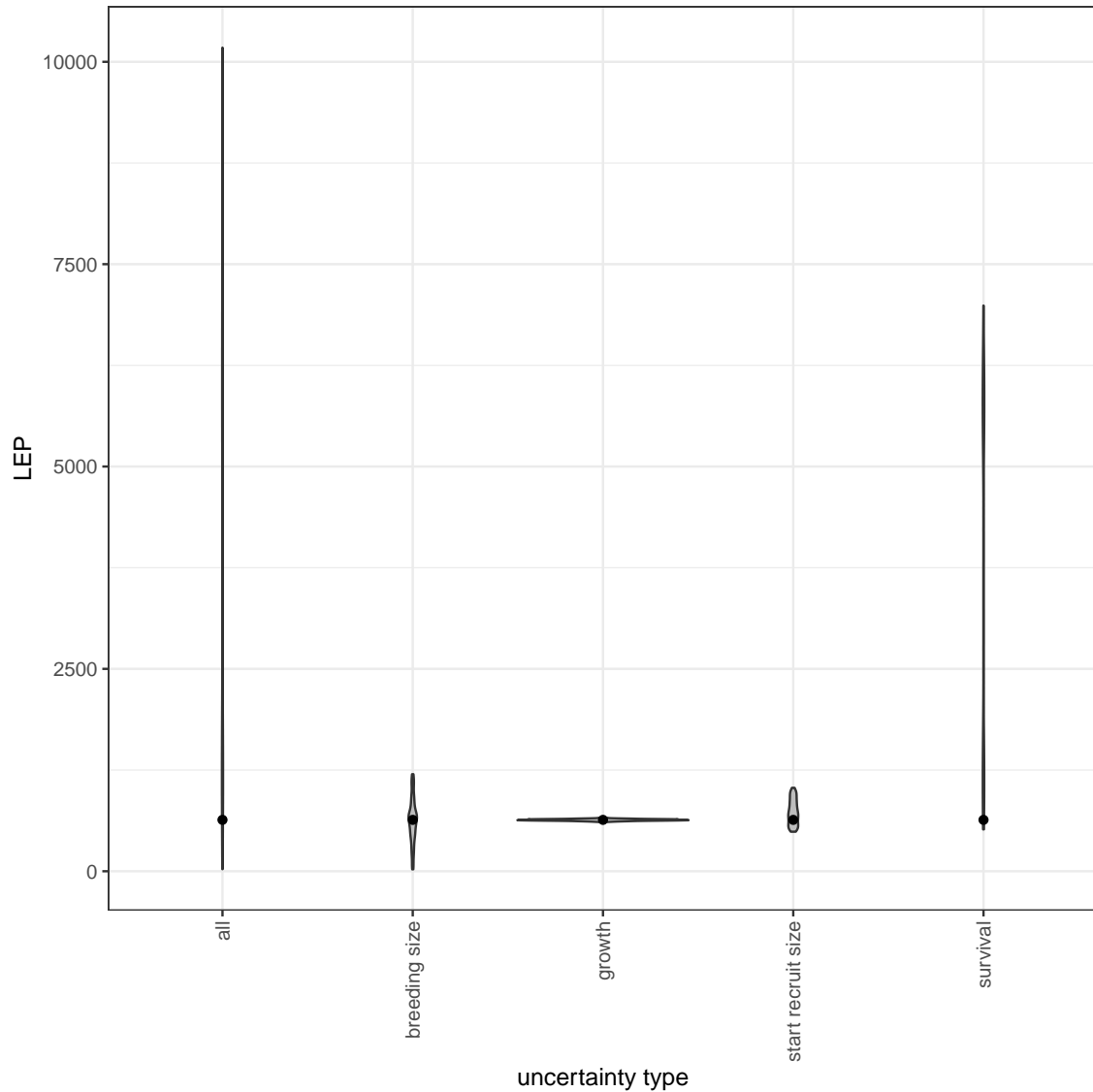


Figure B.7: The contribution of different sources of uncertainty in LEP.

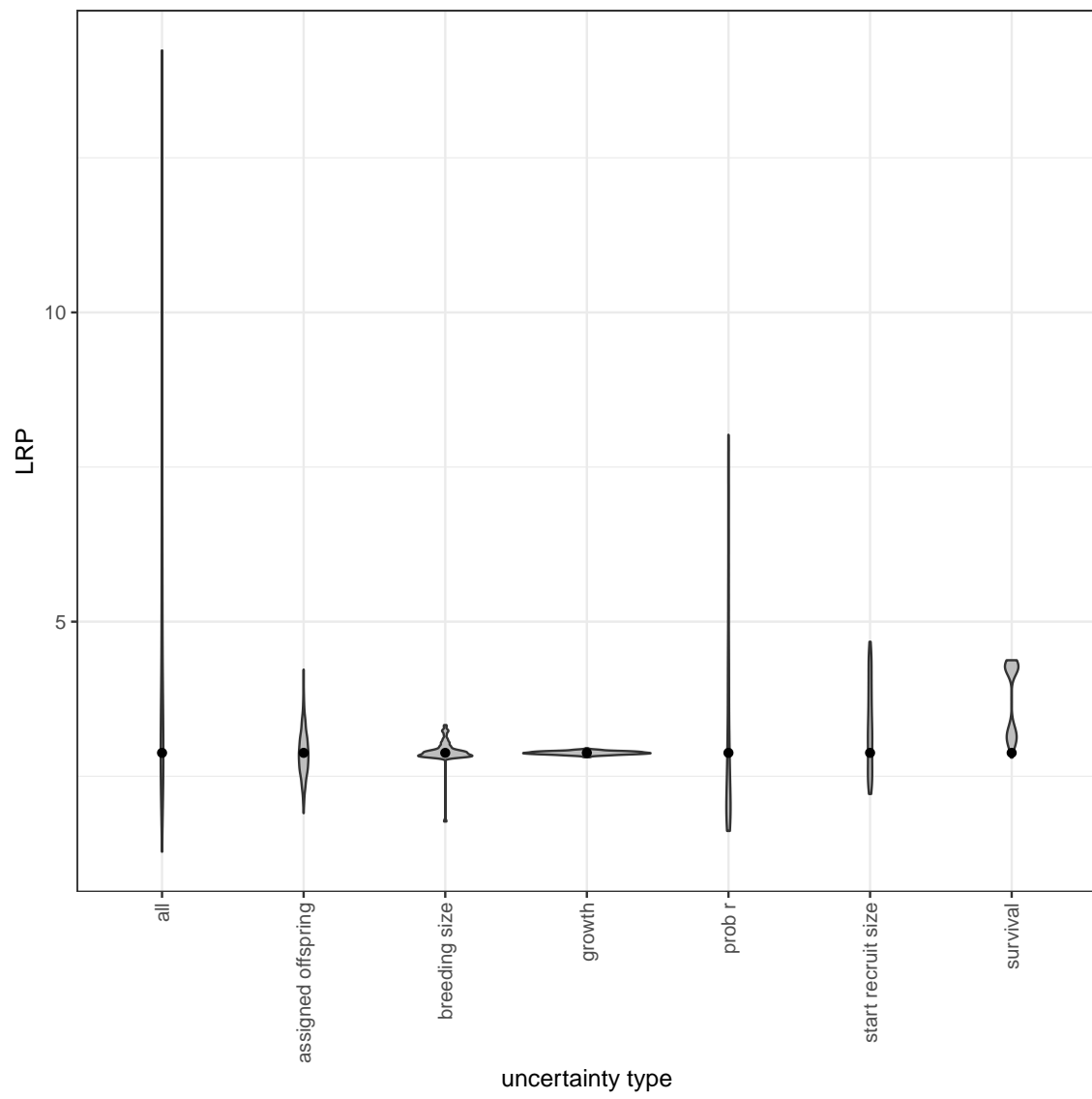


Figure B.8: The contribution of different sources of uncertainty in LRP.

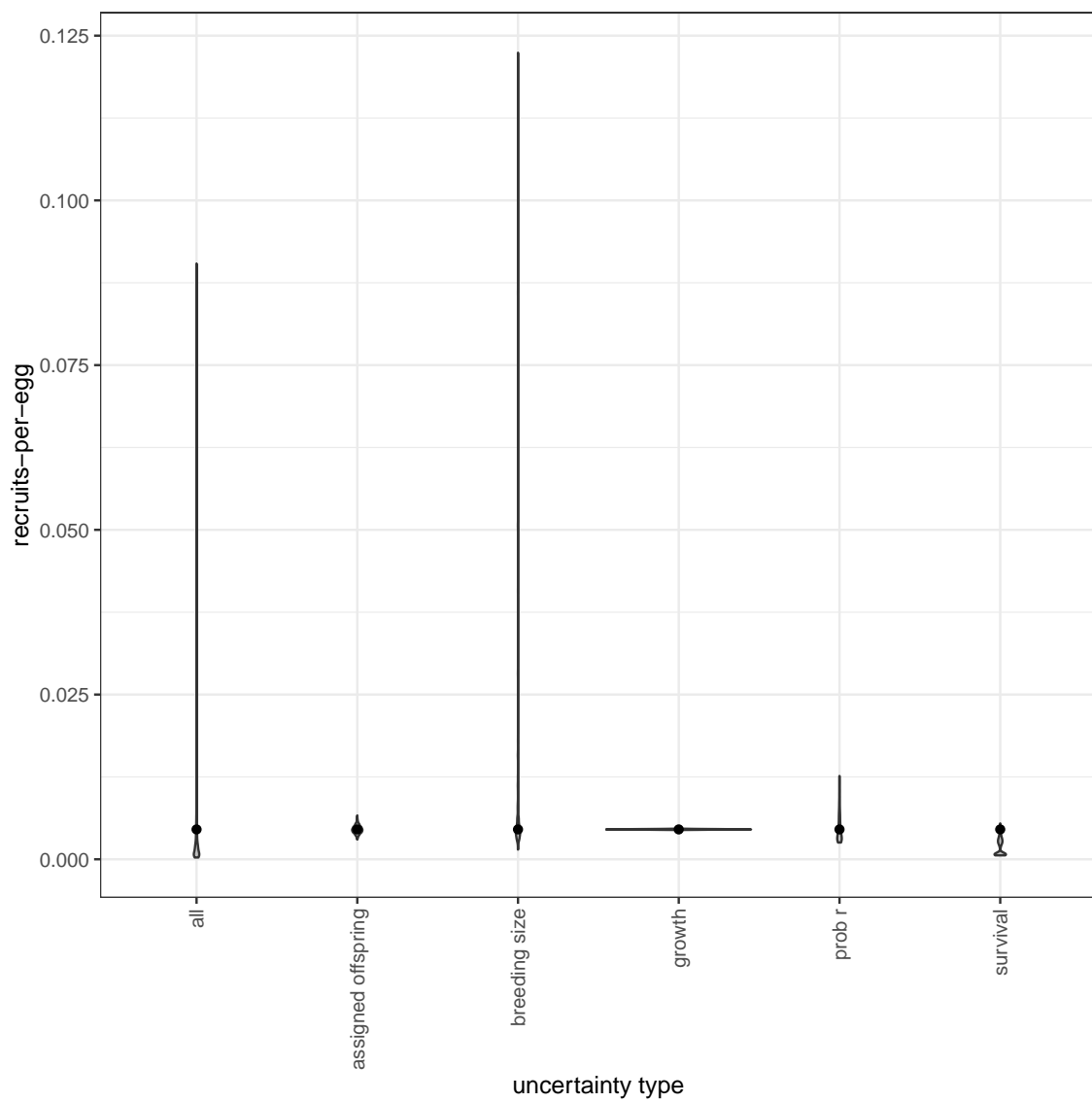


Figure B.9: The contribution of different sources of uncertainty in egg-recruit survival.

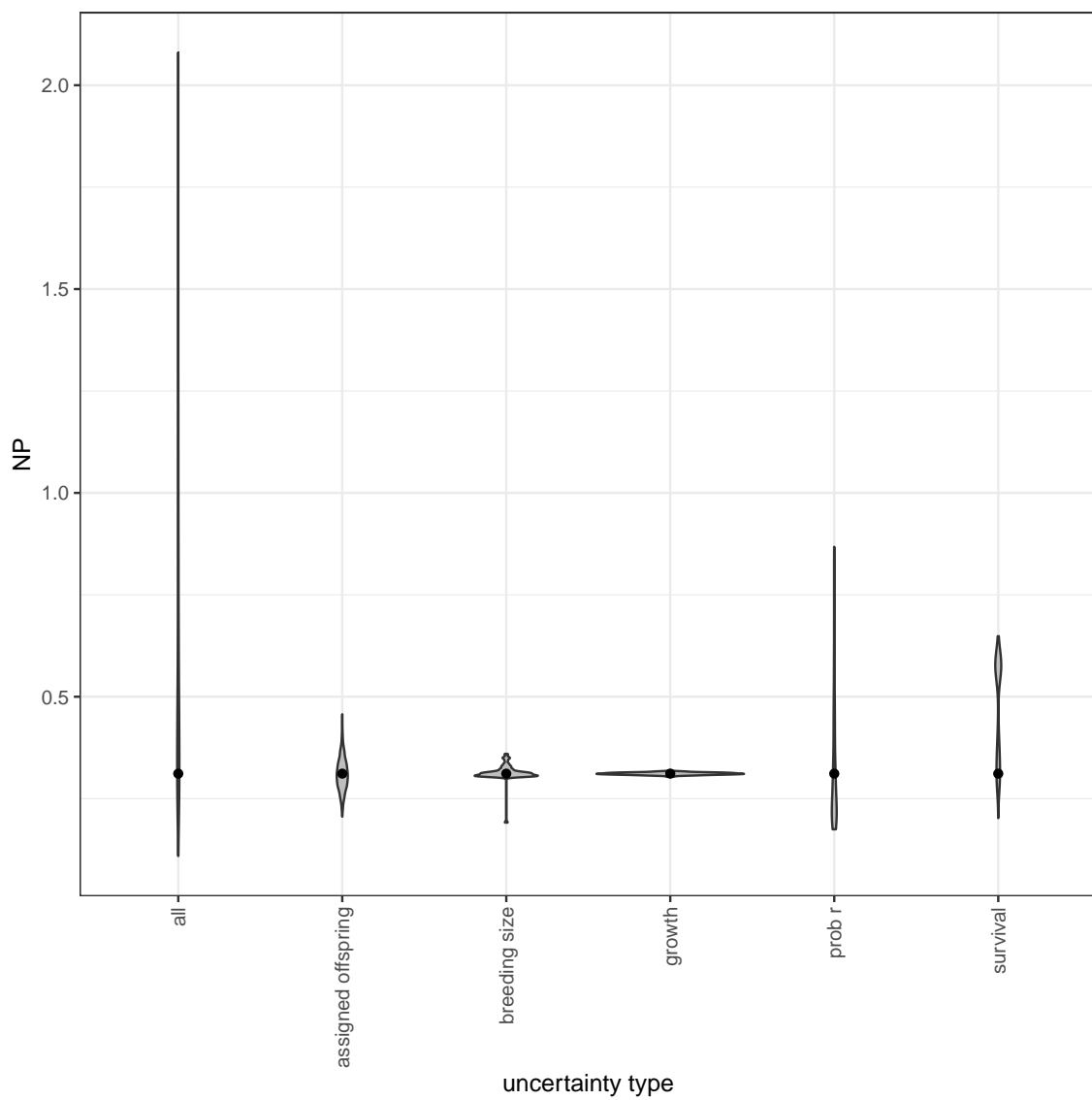


Figure B.10: The contribution of different sources of uncertainty in NP.

References

- Glenn R Almany, Serge Planes, Simon R Thorrold, Michael L Berumen, Michael
609 Bode, Pablo Saenz-Agudelo, Mary C Bonin, Ashley J Frisch, Hugo B Harrison,
Vanessa Messmer, et al. Larval fish dispersal in a coral-reef seascape. *Nature
Ecology & Evolution*, 1:0148, 2017.
- Michael Bode, David H Williamson, Hugo B Harrison, Nick Outram, and Geoffrey P
612 Jones. Estimating dispersal kernels using genetic parentage data. *Methods in
Ecology and Evolution*, 9(3):490–501, 2018.
- L. W. Botsford, J. W. White, M.-A. Coffroth, C. B. Paris, S. Planes, T. L.
615 Shearer, S. R. Thorrold, and G. P. Jones. Connectivity and resilience of coral
reef metapopulations in marine protected areas: matching empirical efforts to
predictive needs. *Coral Reefs*, 28(2):327–337, June 2009. ISSN 0722-4028, 1432-
618 0975. doi: 10.1007/s00338-009-0466-z. URL <http://link.springer.com/10.1007/s00338-009-0466-z>.
- Louis W. Botsford, Alan Hastings, and Steven D. Gaines. Dependence of sustainability on the configuration of marine reserves and larval dispersal distance. *Ecology Letters*, 4:144–150, 2001.
- Scott C Burgess, Kerry J Nickols, Chris D Griesemer, Lewis AK Barnett, Alli-
624 son G Dedrick, Erin V Satterthwaite, Lauren Yamane, Steven G Morgan, J Wilson
White, and Louis W Botsford. Beyond connectivity: how empirical methods can

627 quantify population persistence to improve marine protected-area design. *Ecological Applications*, 24(2):257–270, 2014.

Peter Buston. Forcible eviction and prevention of recruitment in the clown anemonefish. *Behavioral Ecology*, 14(4):576–582, 2003a.

Peter Buston. Social hierarchies: size and growth modification in clownfish. *Nature*, 424(6945):145–146, 2003b.

633 Peter M Buston and Cassidy C DAloia. Marine ecology: reaping the benefits of local dispersal. *Current Biology*, 23(9):R351–R353, 2013.

Peter M Buston and Jane Elith. Determinants of reproductive success in dominant pairs of clownfish: a boosted regression tree analysis. *Journal of Animal Ecology*, 80(3):528–538, 2011.

Peter M Buston, Geoffrey P Jones, Serge Planes, and Simon R Thorrold. Probability 639 of successful larval dispersal declines fivefold over 1 km in a coral reef fish. *Proceedings of the Royal Society of London B: Biological Sciences*, page rspb20112041, 2011.

642 Henry S Carson, Geoffrey S Cook, Paola C López-Duarte, and Lisa A Levin. Evaluating the importance of demographic connectivity in a marine metapopulation. *Ecology*, 92(10):1972–1984, 2011.

645 Hal Caswell. *Matrix population models: construction, analysis, and interpretation*. Sinauer Associates Inc., Sunderland, Massachusetts, 2nd edition, 2001.

- Katrina A Catalano, Allison G Dedrick, Michelle Stuart, Jonathan Purtiz, Humberto
648 Montes, Jr., and Malin Pinsky. Interannual variability of genetic connectivity in
a coral reef fish *Amphiprion clarkii*. in prep.
- R. K. Cowen. Scaling of Connectivity in Marine Populations. *Science*, 311(5760):
651 522–527, January 2006. ISSN 0036-8075, 1095-9203. doi: 10.1126/science.1122039.
URL <http://www.sciencemag.org/cgi/doi/10.1126/science.1122039>.
- Robert K. Cowen and Su Sponaugle. Larval Dispersal and Marine Population Con-
nectivity. *Annual Review of Marine Science*, 1(1):443–466, January 2009. ISSN
654 1941-1405, 1941-0611. doi: 10.1146/annurev.marine.010908.163757. URL <http://www.annualreviews.org/doi/abs/10.1146/annurev.marine.010908.163757>.
- 657 C. C. D'Aloia, S. M. Bogdanowicz, J. E. Majoris, R. G. Harrison, and P. M. Buston.
Self-recruitment in a Caribbean reef fish: a method for approximating dispersal
kernels accounting for seascape. *Molecular Ecology*, 22(9):2563–2572, May 2013.
660 ISSN 09621083. doi: 10.1111/mec.12274. URL <http://doi.wiley.com/10.1111/mec.12274>.
- Cassidy C DAloia, Steven M Bogdanowicz, Robin K Francis, John E Majoris,
663 Richard G Harrison, and Peter M Buston. Patterns, causes, and consequences
of marine larval dispersal. *Proceedings of the National Academy of Sciences*, 112
(45):13940–13945, 2015.
- 666 Augustus J. Fabens. Properties and fitting of the von bertalanffy growth curve.
Growth, 29:265–289, 1965.

- Daphne Gail Fautin, Gerald R Allen, Gerald Robert Allen, Australia Naturalist,
669 Gerald Robert Allen, and Australie Naturaliste. Field guide to anemonefishes and
their host sea anemones. 1992.
- Lysel Garavelli, J Wilson White, Iliana Chollett, and Laurent Marcel Chérubin. Pop-
672ulation models reveal unexpected patterns of local persistence despite widespread
larval dispersal in a highly exploited species. *Conservation Letters*, 11(5):e12567,
2018.
- 675 Sarah O Hameed, J Wilson White, Seth H Miller, Kerry J Nickols, and Steven G
Morgan. Inverse approach to estimating larval dispersal reveals limited population
connectivity along 700 km of wave-swept open coast. *Proceedings of the Royal
678 Society B: Biological Sciences*, 283(1833):20160370, 2016.
- Ilkka Hanski. Metapopulation dynamics. *Nature*, 396(6706):41–49, 1998.
- Deborah R Hart and Antonie S Chute. Estimating von bertalanffy growth parameters
681 from growth increment data using a linear mixed-effects model, with an application
to the sea scallop *placopecten magellanicus*. *ICES Journal of Marine Science*, 66
(10):2165–2175, 2009.
- 684 Alan Hastings and Louis W. Botsford. Persistence of spatial populations depends on
returning home. *Proceedings of the National Academy of Sciences*, 103:6067–6072,
2006a.
- 687 Alan Hastings and Louis W. Botsford. A simple persistence condition for structured
populations. *Ecology Letters*, 9(7):846–852, July 2006b. ISSN 1461-023X, 1461-

0248. doi: 10.1111/j.1461-0248.2006.00940.x. URL <http://doi.wiley.com/10.1111/j.1461-0248.2006.00940.x>.

690

Akihisa Hattori and Yasunobu Yanagisawa. Life-history pathways in relation to gonadal sex differentiation in the anemonefish, *amphiprion clarkii*, in temperate waters of japan. *Environmental Biology of Fishes*, 31(2):139–155, 1991.

693

Kina Hayashi, Katsunori Tachihara, and James Davis Reimer. Low density populations of anemonefish with low replenishment rates on a reef edge with anthropogenic impacts. *Environmental Biology of Fishes*, 102(1):41–54, 2019.

696

J. Derek Hogan, Roger J. Thiessen, Peter F. Sale, and Daniel D. Heath. Local retention, dispersal and fluctuating connectivity among populations of a coral reef fish. *Oecologia*, 168(1):61–71, July 2011. ISSN 0029-8549, 1432-1939. doi: 10.1007/s00442-011-2058-1. URL <http://link.springer.com/10.1007/s00442-011-2058-1>.

702

Jordan N. Holtswarth, Shem B. San Jose, Humberto R. Montes Jr., James W. Morley, and Malin. L Pinsky. The reproductive seasonality and fecundity of yellowtail clownfish (*amphiprion clarkii*) off the philippines. *Bulletin of Marine Science*, 93, 2017.

705

Darren W Johnson, Mark R Christie, Timothy J Pusack, Christopher D Stallings, and Mark A Hixon. Integrating larval connectivity with local demography reveals regional dynamics of a marine metapopulation. *Ecology*, 99(6):1419–1429, 2018.

Jacob P Kritzer and Peter F Sale. *Marine metapopulations*. Elsevier Academic Press, 2006.

711 J.L. Laake. RMark: An r interface for analysis of capture-recapture data with
MARK. AFSC Processed Rep. 2013-01, Alaska Fish. Sci. Cent., NOAA,
Natl. Mar. Fish. Serv., Seattle, WA, 2013. URL [http://www.afsc.noaa.gov/
714 Publications/ProcRpt/PR2013-01.pdf](http://www.afsc.noaa.gov/Publications/ProcRpt/PR2013-01.pdf).

Dale R Lockwood, Alan Hastings, and Louis W Botsford. The effects of dispersal
patterns on marine reserves: does the tail wag the dog? *Theoretical population
717 biology*, 61(3):297–309, 2002.

Anna Metaxas and Megan Saunders. Quantifying the "Bio-" Components in Bio-
physical Models of Larval Transport in Marine Benthic Invertebrates: Advances
720 and Pitfalls. *Biological Bulletin*, 216:257–272, 2009.

Haruki Ochi. Mating behavior and sex change of the anemonefish, *amphiprion clarkii*,
in the temperate waters of southern japan. *Environmental Biology of Fishes*, 26
723 (4):257–275, 1989.

Malin L Pinsky, Humberto R Montes Jr, and Stephen R Palumbi. Using isolation
by distance and effective density to estimate dispersal scales in anemonefish. *Evo-
726 lution*, 64(9):2688–2700, 2010.

Mark Rees, Dylan Z Childs, and Stephen P Ellner. Building integral projection
models: a user's guide. *Journal of Animal Ecology*, 83(3):528–545, 2014.

⁷²⁹ J Roughgarden, S Gaines, and H Possingham. Recruitment dynamics in complex life cycles. *Science*, 241(4872):1460–1466, September 1988. ISSN 0036-8075, 1095-9203. doi: 10.1126/science.11538249. URL <http://www.sciencemag.org/cgi/doi/10.1126/science.11538249>.

⁷³² Steven S. Rumrill. Natural mortality of marine invertebrate larvae. *Ophelia*, 32(1-2):163–198, October 1990. ISSN 0078-5326. doi: 10.1080/00785236.1990.10422030. URL <http://www.tandfonline.com/doi/abs/10.1080/00785236.1990.10422030>.

⁷³⁸ Ocane C. Salles, Jeffrey A. Maynard, Marc Joannides, Corentin M. Barbu, Pablo Saenz-Agudelo, Glenn R. Almany, Michael L. Berumen, Simon R. Thorrold, Geoffrey P. Jones, and Serge Planes. Coral reef fish populations can persist without immigration. *Proceedings of the Royal Society B: Biological Sciences*, 282(1819):20151311, November 2015. ISSN 0962-8452, 1471-2954. doi: 10.1098/rspb.2015.1311. URL <http://rspb.royalsocietypublishing.org/lookup/doi/10.1098/rspb.2015.1311>.

⁷⁴⁴ Jinliang Wang. Sibship reconstruction from genetic data with typing errors. *Genetics*, 166(4):1963–1979, 2004.

⁷⁴⁷ Jinliang Wang. Estimation of migration rates from marker-based parentage analysis. *Molecular ecology*, 23(13):3191–3213, 2014.

J Wilson White, Steven G Morgan, and Jennifer L Fisher. Planktonic larval mortality rates are lower than widely expected. *Ecology*, 95(12):3344–3353, 2014.

750 Jw White, Lw Botsford, A Hastings, and Jl Largier. Population persistence in ma-
rine reserve networks: incorporating spatial heterogeneities in larval dispersal.
Marine Ecology Progress Series, 398:49–67, January 2010. ISSN 0171-8630, 1616-
753 1599. doi: 10.3354/meps08327. URL <http://www.int-res.com/abstracts/meps/v398/p49-67/>.

Adam Yawdoszyn. Fecundity in clownfish. in prep.